Discovery of two 'chimeric' Gastrotricha and their systematic placement based on an integrative approach

ALEXANDER KIENEKE[1,*] and M. ANTONIO TODARO[2]

[1]*Senckenberg am Meer Wilhelmshaven, Deutsches Zentrum für Marine Biodiversitätsforschung, Südstrand 44, 26382 Wilhelmshaven, Germany*
[2]*Department of Life Sciences, Università di Modena e Reggio Emilia, via G. Campi, 213/D, 41125 Modena, Italy*

Sublittoral sand from the islands of Sardinia (Italy) and Flores (Azores) – separated by more than 3700 km linear distance and 8 years between two independent sampling campaigns – yielded conspicuous specimens of two bizarre, yet undescribed, species of the marine gastrotrich clade Macrodasyida. These gastrotrichs combine several character traits that were already known from two, non-related genera. Morphological data were carefully analysed and digitally documented, and nuclear and mitochondrial DNA sequences were used for phylogenetic inference. The results of these analyses claim for the erection of a new genus. Specimens of the new taxon have a body length of less than 400 μm and are characterized by a wide, funnel-shaped mouth opening shielded dorsally by an oral hood and possess a posterior peduncle that ends with a Y-shaped pair of appendages that carry the posterior adhesive tubes. Further tubes occur as anterior, ventrolateral and lateral series; the gonads are unpaired and there is a set of two accessory reproductive organs. Molecular phylogenetic analyses confirm the results of former studies and clearly place the new taxon in Thaumastodermatidae. We hereby propose the establishment of ***Chimaeradasys* gen. nov.** and describe ***C. oligotubulatus* sp. nov.** from the Azores and ***C. polytubulatus* sp. nov.** from Sardinia.

ADDITIONAL KEYWORDS: Azores – biodiversity – integrative taxonomy – Mediterranean Sea – meiofauna – north-eastern Atlantic – new genus – new species – phylogeny – Sardinia.

INTRODUCTION

In the last two decades, phylogenetic studies have profoundly changed our understanding of evolutionary alliances among, and within, traditionally recognized animal taxa. A wave of novelties has also concerned the Gastrotricha, a phylum of minute, acoelomate, aquatic worms. Aquatic ecologists consider gastrotrichs to be permanent and important members of the benthic community known as the meiofauna, but due to their small size and delicate structure, their life habit and biology are largely unknown. Currently, there are more than 850 accepted species of Gastrotricha (WoRMS, 2020), distributed over the two recognized orders Macrodasyida Remane, 1925 (374 marine and four freshwater species) and Chaetonotida Remane, 1925 (132 marine and 348 freshwater species). Across the oceans of the world, gastrotrichs predominantly occur in sandy habitats of the seashore and the shallow sublittoral (Todaro *et al.*, 2019a), but a few species are also reported from the deep sea (Kieneke & Schmidt-Rhaesa, 2015; Kieneke *et al.*, 2020).

In a Linnean framework, gastrotrichs have long been considered a class of the pseudocoelomate Aschelminthes (Schmidt-Rhaesa, 2013; Kieneke & Schmidt-Rhaesa, 2015). By contrast, recent robust phylogenomic studies have shown them to be nested in the Spiralia together with the acoelomate Platyhelminthes in a subclade named Rouphozoa (Struck *et al.*, 2014; Egger *et al.*, 2015). Studies of relationships within Gastrotricha using DNA sequence data analysed with parsimony, maximum likelihood and Bayesian inference have also been useful at resolving the position and classification of

*Corresponding author. E-mail: alexander.kieneke@senckenberg.de

problematic taxa. In this regard, the study by Todaro *et al.* (2012) may be regarded as paradigmatic. They (1) could robustly place the puzzling *Redudasys fornerise* Kesielwski, 1987 to the evolutionary tree of Gastrotricha, at that time one of the only two freshwater representatives of the entire order Macrodasyida, (2) erected a new genus to allow a better reclassification of its likely sister-taxon, the marine *Anandrodasys agadasys* (Hochberg, 2003), (3) created a new high-ranking taxon, Redudasyidae, to allocate members of the newly discovered clade and (4) confirmed the previously hypothesized colonization of freshwater ecosystems by Gastrotricha to have occurred at least twice independently (freshwater colonization of Macrodasyida apart from that of Chaetonotida, see: Kisielewski, 1990, Todaro *et al.*, 2012).

Undoubtedly, most of the current phylogenetic novelties have emerged from analyses based on molecular markers. However, the main goal of these studies has always been the search for congruence between phylogenetic hypotheses either based on morphological or on molecular data. In some instances, congruence could only be demonstrated after additional morphological surveys. For example, the genus *Megadasys* Schmidt, 1974 has been transferred from Cephalodasydae Hummon & Todaro, 2010 to Planodasyidae Rao & Clausen, 1970 based on the results of new investigations on its reproductive apparatus and spermatozoa, which have been shown to bear previously undetected similarities/homologies with the same traits of the planodasyid taxon *Crasiella* Clausen, 1968 (Guidi *et al.*, 2014). On other occasions, DNA sequence data have induced a reinterpretation of morphological traits that resulted in a reclassification of taxa as, for example, in the recent case of several species previously affiliated to the genus *Macrodasys* Remane, 1924. As a result of an integrated study, these species had to be moved to a newly erected genus named *Kryptodasys* Todaro, Dal Zotto, Kånneby, Hochberg, 2019 (see: Todaro *et al.*, 2019b). In yet other circumstances, full congruence between phylogenetic hypotheses based on molecular data and morphological characters could not be achieved, as in the case of *Thaidasys tongiorgii* Todaro, Dal Zotto & Leasi, 2015. However, morphological evidence is not in contrast with results from molecular data (Todaro *et al.*, 2015).

Molecular phylogenetic analyses of the recent past have, furthermore, demonstrated their strength when completely new 'morphotypes' of Gastrotricha are discovered and have to be integrated into the phylogenetic system. Sometimes, phylogenetic information content of morphological traits is not recognized immediately or, alternatively, different taxonomists assign different significance to the same characters. This is especially true if new forms exhibit new combinations of traits that are otherwise already known from existing taxa. Notwithstanding the presence of further characters that could have claimed an alternative systematic position, such known traits were frequently used for affiliating the new forms to already known taxa. This may cause the well-known 'wastebasket taxon effect' (e.g. Plotnick & Wagner, 2006), in which species/genera with superficial resemblance are affiliated to the same higher ranking taxon (genus/family). Within Gastrotricha, the macrodasyidan family Cephalodasyidae (formerly Lepidodasyidae), for instance, still includes several genera that do not share clear synapomorphies (Hummon & Todaro, 2010). Another striking example is the recently discovered *Hummondasys jamaicensis* Todaro, Leasi & Hochberg, 2014. Based on general morphology, it would have probably been assigned to either Turbanellidae or to Cephalodasyidae. However, molecular-based phylogenetic reconstruction negated both options and the erection of the new family Hummondasyidae was proposed following a careful review of the external and internal anatomy (Todaro *et al.*, 2014).

Based on these preconditions, we here present the descriptions of two new species bearing a 'chimeric morphology'. We found their systematization on congruence between morphological and molecular data analyses. Specimens of the two new species were discovered by the two authors during independent research on meiofaunal organisms in the Azores and Sardinia.

MATERIAL AND METHODS

SAMPLING AND EXTRACTION OF MEIOFAUNA

Azores (AK)

The sediment sample that contained the new species from the Azores was sampled during the cruise M150 of the German research vessel *Meteor* (George *et al.*, 2018; Kieneke, 2018; Kieneke *et al.*, 2018). At station 84-1 (39°19.699'N, 031°16.390'W, about 6 km to the south-west of the Azorean island Flores), a Shipek grab was lowered to 257 m water depth on 3 September 2018. One subsample of the sediment was used for *in situ* extraction and fixation of anaesthetized meiofauna aboard, while the other subsample (about 400 mL of fine sand) was filled into a 2.5-L PE bucket, covered with approximately 1.5 L of filtered ambient seawater and ventilated via a standard pump for fish-keeping purposes. The live sample was stored in the cool room of R/V *Meteor* at 10 °C for the remaining cruise until extraction of live meiofauna at the Universidade dos Açores, Marine Palaeo-Biogeography Laboratory (Sérgio P. Ávila). Time-span from sampling until

extraction of meiofauna was 31 days in the case of sample 84-1. Extraction of living meiofauna was carried out using the anaesthetization–decantation extraction method (Pfannkuche & Thiel, 1988; Kieneke *et al.*, 2020) with a 7% (w/v) aqueous solution of $MgCl_2$ and a 40-µm sieve. The retained meiofauna was rinsed into a Petri dish using filtered, ambient seawater. The sample was screened for gastrotrich individuals using a Wild M5 dissecting microscope equipped with transmitted light illumination.

Sardinia (MAT)

The Mediterranean species was collected during a 10-day workshop on soft-bodied meiofauna held at La Maddalena Marine National Park (northern Sardina, Italy) in September 2010 (Curini *et al.*, 2012). The sediment containing the single specimen of the new species was collected on 4 September 2010 by scuba-diving at a depth of 35 m at Costa Paradiso, Sardinia, Italy (41°3'8.84"N, 8°56'15.71"E). Meiofaunal specimens were extracted from sediment by the narcotization–decantation technique, using a 7% $MgCl_2$ solution, as described above. However, the supernatant was poured directly into a 5-cm diameter Petri dish (i.e. without sieving and rinsing with seawater) and searched for Gastrotricha under a Wild M8 dissecting microscope (Todaro & Hummon, 2008; Todaro *et al.*, 2019a).

MICROSCOPY, IMAGING AND MEASUREMENTS

Single specimens were sucked from the sample for further processing using a capillary glass pipette or a micropipette, placed on a microscopic slide with a small drop of $MgCl_2$ solution and covered with a cover glass. Microscopic investigation and photographic documentation was performed either with an Olympus BX 53 compound microscope equipped with differential interference contrast (DIC) and an attached digital camera Olympus PEN E-PL5 (specimen from Flores), or with a Leitz Dialux 20 microscope (Nomarski/DIC) with a mounted Nikon Digital Sight DSFi1 digital camera driven by the Nikon Nis-F v.4 software (specimen from Sardinia).

Calibrated digital images were used for measurements carried out with Fiji (ImageJ 1.51n; Schindelin *et al.*, 2012; Rueden *et al.*, 2017). Drawings of the holotype specimens are based on the images of the anaesthetized animals and were carried out with Adobe Illustrator CS5. The descriptions of the new species follow the convention as suggested by Hummon *et al.* (1992, 1993). According to this, positions of different morphological features are given in percentage units (U) of total body length measured from anterior to posterior.

DNA SEQUENCING

After microscopic investigation, the cover glass was floated by adding an excess of $MgCl_2$ solution and removed afterwards. The specimen from the Azores was recovered with a pipette, briefly rinsed with deionized water and then transferred to a 0.2-mL PCR reaction vial with a minimum volume of water. The specimen from Sardinia was likewise recovered from the slide but stored in 95% ethanol for later use. In order to extract the genomic DNA, 35 µL of InstaGene Matrix (catalog # 732–6030, Bio Rad Laboratories, Hercules, USA) was added to each vial and processed after the manufacturer's manual (see: Kieneke & Nikoukar, 2017). In the case of the Sardinian specimen, the ethanol was evaporated beforehand. For each PCR reaction, 1 µL of the InstaGene-extraction was used as template DNA. The PCR reactions were prepared using illustra PuReTaq Ready-To-Go PCR beads (GE Healthcare UK, Little Chalfont, UK) with 1 µL of template DNA, 1 µL of forward and reverse primer at 10 pmol/L, respectively, and 22 µL of H_2O for molecular purposes (Carl Roth GmbH, Karlruhe, Germany). An approximately 650-bp long fragment of the mitochondrial cytochrome *c* oxidase subunit I gene (*COI*mtDNA) and an about 1800-bp long fragment of the nuclear encoded 18S ribosomal RNA-gene (18S rDNA) were amplified using the primer combinations and thermal cycler regimes as presented in Table 1. An Eppendorf Mastercycler pro S (Eppendorf AG, Hamburg, Germany) was used for PCR. Purification of the PCR products was either carried out through Macrogen Europe Laboratory (*COI*) or by using ExoSAP-IT PCR Product Cleanup Reagent (Thermo Fisher Scientific, Waltham, USA) according to the manufacturer's manual (18S). Sequencing of the amplicons was carried out through Macrogen Europe Laboratory (Amsterdam, Netherlands). Any effort to amplify the targeted genes of the Sardinian specimen failed so far. However, the extracted DNA of both specimens is stored at –20 °C in the DNA collection of the first author.

PHYLOGENETIC ANALYSES

The ABI-format sequence (chromatogram) files delivered from Macrogen Europe Laboratory were quality controlled and pre-edited with Finch TV v.1.4.0 (Geospiza Inc., Seattle, WA, USA). Assembly of contigs was executed with GENEIOUS PRO 5.3.3 (Biomatters Inc., Auckland, New Zealand), including further quality control and sequence editing, if necessary. For assembling the dataset of almost complete 18S rDNA sequences, the single sequence of the Azorean specimen was added to the existing data matrix of Todaro *et al.* (2019b). The final alignment was obtained using MUSCLE (Edgar, 2004)

Table 1. Primers used in this study and their respective direction, sequence and usage.

Primer	Direction	Sequence 5' to 3'	Usage for	Reference
18S primers				
18SE-**M13F**	forward	**GTAAAACGACGGCCAGT**CTGGTTG ATCCTGCCAGT	PCR/seq.	Hillis & Dixon (1991); see Blanco-Berical *et al.* (2011)
18SL-**M13R-pUC**	reverse	**CAGGAAACAGCTATGAC**CACCTAC GGAAACCTTGTTACGACTT	PCR/seq.	Hamby & Zimmer (1988); see Blanco-Berical *et al.* (2011)
PCR regime 18SE/18SL		4 min at 95 °C, 38× (0.75 min at 95 °C, 1 min at 51 °C, 2 min at 72 °C), 4 min at 72 °C		
F-566	forward	CAGCAGCCGCGGTAATTCC	sequencing	Hadziavdic *et al.* (2014)
R-1200	reverse	CCCGTGTTGAGTCAAATTAAGC	sequencing	Hadziavdic *et al.* (2014)
COI **primers**				
LCO1490	forward	GGTCAACAAATCATAAAGATATTGG	PCR/seq.	Folmer *et al.* (1994)
HCO2198	reverse	TAAACTTCAGGGTGACCAAAAAATCA	PCR/seq.	Folmer *et al.* (1994)
PCR regime LCO1490/ HCO2198		3 min at 94 °C, 38x (0.5 min at 94 °C, 1 min at 48 °C, 1 min at 72 °C), 7 min at 72 °C		

Bold sequences: 5'-tails M13F/M13R-pUC for sequencing.

with default setting and as implemented in the software package MEGA X (Kumar *et al.*, 2018). It consists of 49 sequences in total, originating from 46 different species of Macrodasyda, plus one sequence of the paucitubulatinan *Xenotrichula intermedia* Remane, 1934 (as outgroup) and the newly obtained sequence of the Azorean specimen. The dataset covers 26 genera of the currently known ten families of Macrodasyida (Table 2) and consist of 1877 positions. The *COI* sequence of the Azorean species was aligned with further gastrotrich sequences obtained from public repositories (Supporting Information, Table S1) by the aid of the software MEGA X (Kumar *et al.*, 2018) using the ClustalW algorithm for multiple-sequence alignment (Thompson *et al.*, 1994). The sequences were aligned based on the codons and using the default settings for ClustalW. Afterwards, it was further optimized with the alignment editor of MEGA X based on the translated amino acids. The final alignment consists of 73 sequences from 39 species of 15 genera of the Macrodasyida, including the new Azorean species and one sequence of *Xenotrichula intermedia* as outgroup. Some sequences included are tagged as 'cytochrome-c-oxidase subunit I gene-like' (JF432020, JF432021, JF432022, JF432025, JF432033, JF432034, JF432038, JF432045; see Table S1), i.e. they could represent mitochondrially derived nuclear genes (Todaro *et al.*, 2011). A translation into amino acid sequences using the 'invertebrate mitochondrial' code indeed yielded stop-codons in these doubtful sequences. One such *COI*-like sequence of the

species *Ptychostomella tyrrhenica* Hummon *et al.*, 1993 (JF432027) was completely excluded from our analysis because it created an extremely long branch after initial calculations. Furthermore, at least one 'gastrotrich' *COI*-sequence (JF432035, *Tetranchyroderma* sp. 3) was recently identified as a possible bacterial sequence (Mioduchowska *et al.*, 2018) and was, therefore, also excluded from the analysis. The final alignment comprises 774 positions, including the alignment gaps (indels).

The 18S dataset was subsequently converted into both interleaved Fasta and Nexus formatted files and analysed using three different approaches: maximum likelihood (ML), maximum parsimony (MP) and Bayesian inference (BI). Maximum likelihood and MP were executed with MEGA X; for BI, the software MrBayes 3.1.2 (Ronquist & Huelsenbeck, 2003) was used. As evolutionary model for nucleotide substitution for the ML and BI analyses, the GTR+G+I model (Nei & Kumar, 2000) was used because it was the most favoured by both the AICc and the lnL criteria in MrModelTest v.2.3 (Nylander, 2004) and MEGA X. Maximum likelihood analysis started with an initial tree calculated from a matrix of pairwise distances with the Neighbor-Joining (NJ) method (Saitou & Nei, 1987), and the tree with the highest log-likelihood was retained. Maximum parsimony analysis ran using the subtree-pruning-recrafting algorithm for branch swapping (Nei & Kumar, 2000) and the tree with

Table 2. Gastrotrich 18S rDNA sequences used in the phylogenetic analyses. Species, accession numbers, geographic origin and reference

Taxon	Accession	Origin	Reference
Cephalodasyidae			
Cephalodasys sp.1	AY963691	White Sea, Russia	Petrov *et al.*, 2007
Dolichodasys sp. 1	AM231778	San Isidoro, Italy	Todaro *et al.*, 2006
Mesodasys laticaudatus	JF357657	Albinia, Italy	Todaro *et al.*, 2011
Mesodasys littoralis	JF357658	Bou Ficha, Tunisia	Todaro *et al.*, 2011
Paradasys sp. 1	AM231781	Ionian sea, Italy	Todaro *et al.*, 2006
Pleurodasys helgolandicus	JN203486	Ibiza, Spain	Todaro *et al.*, 2012
Dactylopodolidae			
Dactylopodola cf. *baltica*	JF357650	Ras Alard, Kuwait	Todaro *et al.*, 2011
Dactylopodola mesotyphle	JF357651	Punta Ala, Italy	Todaro *et al.*, 2011
Dactylopodola typhle	JF357652	Bou Ficha, Tunisia	Todaro *et al.*, 2011
Dactylopodola typhle	JF357653	Torre Civette, Italy	Todaro *et al.*, 2011
Hummondasyidae			
Hummondasys jamaicensis	KM083602	Negril, Jamaica	Todaro *et al.*, 2014
Lepidodasyidae			
Lepidodasys unicarenatus	JF357665	Pianosa, Italy	Todaro *et al.*, 2011
Macrodasyidae			
Kryptodasys macrocurinii	MK880150	Sardinia, Italy	Todaro *et al.*, 2019b
Kryptodasys ulfjondeliusi	MK880151	Gullmarsfiord, Sweden	Todaro *et al.*, 2019b
Macrodasys sp. 1	JF357654	Torre Civette, Italy	Todaro *et al.*, 2011
Macrodasys sp. 2	JF357670	Bohuslän, Sweden	Todaro *et al.*, 2011
Thaidasys tongiorgii	KR072683	Phuket Island, Thailand	Todaro *et al.*, 2015
Urodasys sp. 1	DQ079912	Florida, USA	Sørensen *et al.*, 2006
Urodasys sp. 2	AY218102	NA	Giribet *et al.*, 2004
Planodasyidae			
Crasiella sp.1	JN203488	Ilhabela, Brazil	Todaro *et al.*, 2012
Megadasys sp. 1	JF357656	Porto Cesareo, Italy	Todaro *et al.*, 2011
Megadasys sp. 2	JF357655	Grotta del Ciolo, Italy	Todaro *et al.*, 2011
Redudasyidae			
Anandrodasys agadasys	JN203487	St. John Island, USA	Todaro *et al.*, 2012
Redudasys fornerise	JN203489	Represa do Broa, Brazil	Todaro *et al.*, 2012
Thaumastodermatidae			
Acanthodasys sp. 1	JF357638	Capraia, Italy	Todaro *et al.*, 2011
Acanthodasys aculeatus	JF357639	Capraia, Italy	Todaro *et al.*, 2011
Chimaeradasys oligotubulatus	LR862428	Ilha das Flores, Azores	present study
Diplodasys ankeli	JF357624	Meloria Shoals, Italy	Todaro *et al.*, 2011
Diplodasys meloriae	JF357640	Meloria Shoals, Italy	Todaro *et al.*, 2011
Oregodasys ocellatus	JF357642	Meloria Shoals, Italy	Todaro *et al.*, 2011
Oregodasys ruber	JF357625	Meloria Shoals, Italy	Todaro *et al.*, 2011
Oregodasys tentaculatus	JF357626	Meloria Shoasl, Italy	Todaro *et al.*, 2011
Pseudostomella etrusca	JF357633	Albinia, Italy	Todaro *et al.*, 2011
Ptychostomella lamelliphora (=sp1)	JF357643	Ilhabela, Brazil	Todaro *et al.*, 2011
Ptychostomella tyrrhenica	JF357634	Albinia, Italy	Todaro *et al.*, 2011
Tetranchyroderma esarabdophorum	JF357627	Mahdia, Tunisia	Todaro *et al.*, 2011
Tetranchyroderma hirtum	JF357628	Capraia, Italy	Todaro *et al.*, 2011
Tetranchyroderma papii	JF357637	Sardegna, Italy	Todaro *et al.*, 2011
Tetranchyroderma thysanophorum	JF357630	Albinia, Italy	Todaro *et al.*, 2011

Table 2. Continued

Taxon	Accession	Origin	Reference
Thaumastoderma moebjergi	JF357671	Bohuslän, Sweden	Todaro *et al.*, 2011
Thaumastoderma ramuliferum	JF357631	Meloria Shoals, Italy	Todaro *et al.*, 2011
Turbanellidae			
Paraturbanella dohrni	JF357659	Punta Ala, Italy	Todaro *et al.*, 2011
Paraturbanella pallida	JF357660	Capraia, Italy	Todaro *et al.*, 2011
Paraturbanella teissieri	JF357661	Punta Ala, Italy	Todaro *et al.*, 2011
Turbanella bocqueti	JF357662	Tramore, Ireland	Todaro *et al.*, 2011
Turbanella cornuta	JF357663	Chioggia, Italy	Todaro *et al.*, 2011
Turbanella lutheri	JF357669	Torö, Sweden	Todaro *et al.*, 2011
Xenodasyidae			
Xenodasys riedli	JN203490	St. John Island, USA	Todaro *et al.*, 2012
Xenotrichulidae*			
Xenotrichula intermedia	JF357664	Mahdia, Tunisia	Todaro *et al.*, 2011

* Order Chaetonotida; NA, not available.

the least number of evolutionary steps was kept. For both, ML and MP analyses, all sites of the alignment, including the gap-containing sites, were used. The BI tree search operated with two parallel runs and four independent Markov chains per run. The analysis ran for 10 000 000 generations and sampled trees every 100th generation. To obtain a consensus tree, we used all the trees generated after the two parallel runs reached equilibrium in their standard deviation, which occurred after about 25 000 generations. Therefore, the first 250 sampled trees were discarded. From the 99 750 retained trees, a 50% consensus tree was produced with TreeView (Page, 1996).

The alignment of partial mitochondrial *COI* sequences was converted into Nexus format and analysed with MrModelTest v.2.3 (Nylander, 2004) and PAUP* 4.0 (Sinauer Associates, Inc., Sunderland, USA) in order to estimate the best-fit model for nucleotide substitution. Both the hierarchical likelihood ratio test and the Akaike information criterion favoured the GTR+G+I model, which was used for a ML analysis carried out with MEGA X. The ML analysis started with an initial NJ tree obtained from a matrix of pairwise distances calculated by MEGA X using the MCL approach. The final alignment of the *COI* sequences contained 774 positions. However, all alignment positions with gaps were deleted before analysis, which resulted in a final dataset of 381 positions.

In order to estimate robustness of received clades, the bootstrap test (Felsenstein, 1985) was applied in conjunction with ML analysis of the 18S and *COI* datasets and with the MP analysis of the 18S alignment. Each analysis ran with 1000 replications, respectively.

RESULTS

MOLECULAR PHYLOGENETIC ANALYSES

All trees obtained by the different analyses based on the 18S ribosomal RNA gene (ML, MP and BI; see Figs 6–8) yield almost identical results. Beside the monogeneric families, currently recognized taxa like Planodasyidae, Redudasyidae and the densely sampled Turbanellidae and Thaumastodermatidae are revealed as monophyletic groups with either high bootstrap or posterior probability values, respectively. Likewise, both thaumastodermatid subgroups, Thaumastodermatinae and Diplodasyinae, as well as most genera that were represented by more than a single species, receive high nodal support. Among this is *Dactylopodola* Strand, 1929 (family Dactylopodolidae), represented in the analyses by four terminals. In contrast, some traditional families such as Macrodasyidae and Cephalodasyidae decay into two or multiple lineages, respectively. Most important, the sequence of the specimen from the Azores unequivocally clusters in Thaumastodermatinae with the most derived taxa such as *Pseudostomella* Swedmark, 1956, *Ptychostomella* Remane, 1926 and *Tetranchyroderma* Remane, 1926.

The tree that was obtained from the ML analysis based on the alignment of the *COI* dataset (Supporting Information, Fig. S1) supports all species that are included with more than a single specimen as monophyletic. All of these, apart from *Turbanella cornuta* Remane, 1925, furthermore receive high bootstrap support values. Likewise, many genera that are represented with more than a single species receive high support as monophyletic groups, i.e. *Dactylopodola*, *Diplodasys* Remane, 1927, *Macrodasys*

Remane, 1924, *Megadasys* Schmidt, 1974, *Mesodasys* Remane, 1951, *Oregodasys* Hummon, 2008, *Redudasys* Kisielewski, 1987. However, the quantitatively best represented genera, *Tetranchyroderma*, Remane, 1926 *Turbanella* Schultze, 1853 and *Urodasys* Remane, 1926 decay into multiple lineages. The sequence of the new Azorean species clusters with the sequence of *Tetranchyroderma quadritentaculatum* Todaro *et al*., 1992 (JF432024) with high bootstrap support.

TAXONOMIC ACCOUNT

PHYLUM GASTROTRICHA METSCHNIKOFF, 1865

ORDER MACRODASYIDA REMANE, 1925 (RAO & CLAUSEN, 1970)

FAMILY THAUMASTODERMATIDAE REMANE, 1927

SUBFAMILY THAUMASTODERMATINAE REMANE, 1927 (RUPPERT, 1978)

GENUS *CHIMAERADASYS* GEN. NOV.

Zoobank registration: urn:lsid:zoobank.org:act:832074E4-FCC0-410F-85FB-2AFFCFEC637E

Genus type species: Chimaeradasys oligotubulatus sp. nov.

Diagnosis: A thaumastodermatin characterized by a smooth cuticle and a forked caudal peduncle. Body slender, slightly arched dorsally and flattened ventrally; adults up to 391 µm in total length (TL) and up to 74 µm in maximum width. Head furnished with ample mouth and oral hood but lacking sensory structures, such as knob-like organs and eye spots. Sensorial (?) papillae present on mouth rim and margins of the oral hood. Trunk widest in the mid-intestinal region, tapering gently to the rear before ending abruptly in a peculiar, narrow caudal peduncle; peduncle branched, indenting medially at U93. Five to eight pairs of large epidermal glands along the pharyngeal and posterior trunk region, other smaller glands may be present along the anterior trunk region.

Numerous sensorial cilia are distributed in lateral and dorsolateral columns along the body, sparingly around the head. Locomotor cilia arranged in transverse bands, covering the entire ventral surface, except the anal region and peduncle. Anterior adhesive tubes (TbA), one or two per side, in a row just posterior to the mouth; ventral adhesive tubes (TbV) absent or present as a single pair in the anterior pharyngeal region; lateral adhesive tubes (TbL), noticeable, one per side just anterior to the peduncle; ventrolateral adhesive tubes (TbVL), five to ten per side, one of which is in the anterior pharyngeal region and the others distributed along the half to two-thirds of the trunk; dorsal adhesive tubes (TbD) absent; posterior adhesive tubes (TbP), three per side, two of which are at the end of each peduncular branch and one flanking them medially. Mouth wide, (up to 55 µm in breadth), leading to a shallow, funnel-shaped buccal cavity and surmounted dorsally by a scalloped oral hood. Pharynx up to 92 µm in length; pharyngeal pores near the base, with ventrolateral openings at U28–U33. Pharyngeo-intestinal junction (PhIJ) at U32–U34, intestine straight, slightly wider at midbody; anal opening ventral at U80–U88. Hermaphrodite; single testis on right body side, elongate, beginning posterior to the PhIJ; sperm duct presumably opens on the ventral surface, through the anus or near to it; spermatozoa filiform with a corkscrew-like anterior region and a lash-like tail. Ovary solitary, posterior in the trunk region; eggs growing from posterior to anterior with the ripest cell dorsal to the mid-intestine. Caudal organ, compact, posterior to the ovary, glandomuscular in nature, showing several spermatozoa, probably to be released ventrally throughout an independent pore or via the anus; frontal organ inconspicuous, sac-like, at midline, adjacent to the caudal organ, with several motile spermatozoa inside. Anatomical and/or functional relationship between testis and the accessory reproductive organs or between the latter structures, indefinite. *Type species: Chimaeradasys oligotubulatus*; other species: *C. multitubulatus*.

Etymology: The new genus name is derived from the Greek Χίμαιρα (Latinized as *Chimaera*), a mythological creature composed of a lion, a goat and a snake, and from the Greek δασύς, shaggy, which refers to the dense facing with cilia of the ventral surface of Gastrotricha and which is often used as the second part of generic names of Macrodasyida.

Both authors independently found specimens of the new genus, although with almost exactly eight years between the discoveries, and both faced the challenge of a proper systematic placement, because the animals appeared as 'chimeras', showing characters of several genera of the Macrodasyida, viz. *Dendrodasys* Wilke, 1954 and *Ptychostomella* (see 'Taxonomic affinities' for more details).

CHIMAERADASYS OLIGOTUBULATUS SP. NOV.

(FIGS 1, 2)

Zoobank registration: urn:lsid:zoobank.org:act:4871880A-8688-4883-A5DB-C2FE600C389

Type locality: Portugal, Azores, Flores, sandy deep sublittoral bottom at about 6 km to the south-west of the southern coast (station #84-1, 39°19.699'N, 031°16.390'W); collection made on 3 September 2018 with a Shipek Grab lowered to a depth of 257 m from aboard the R/V *Meteor* during expedition M150.
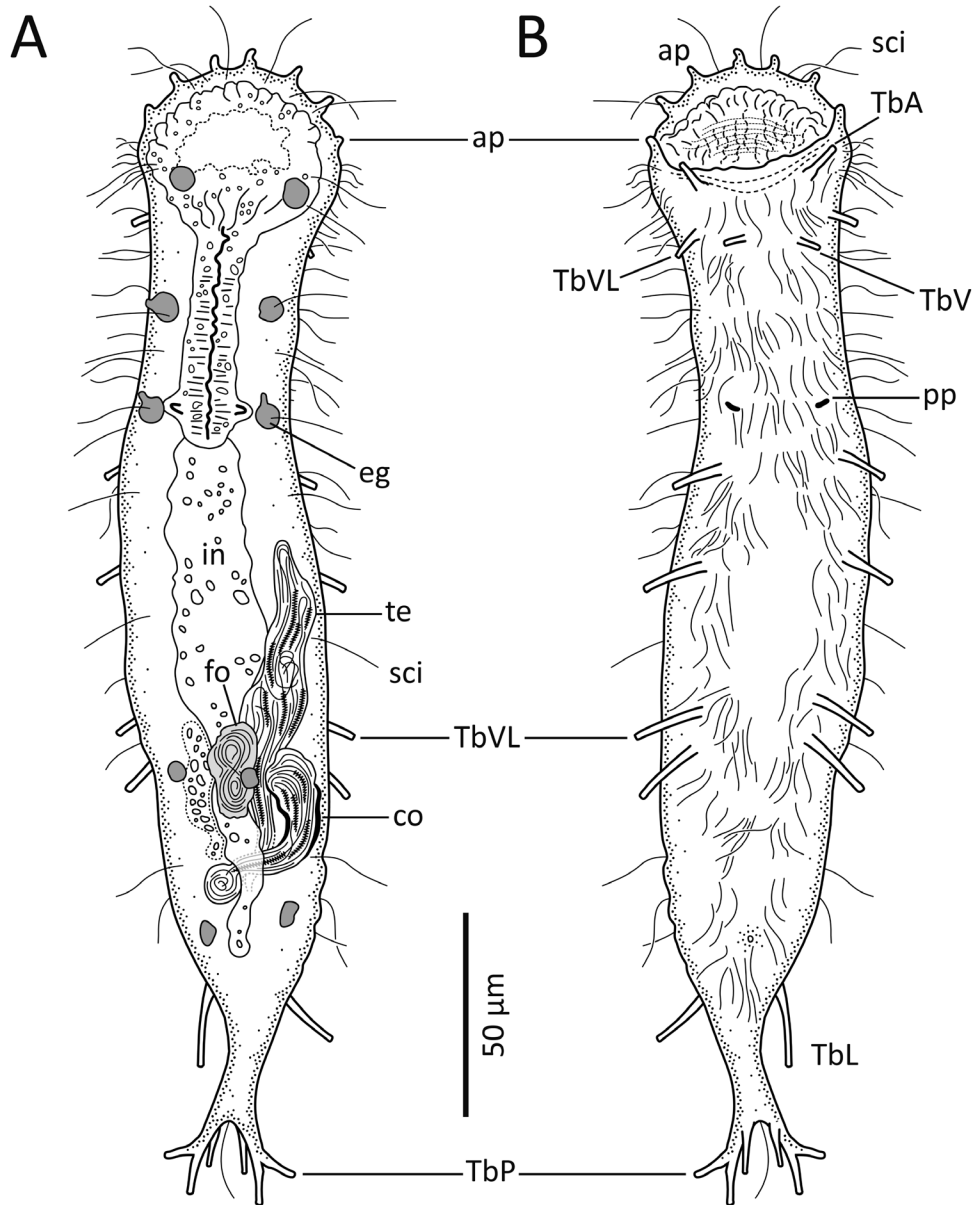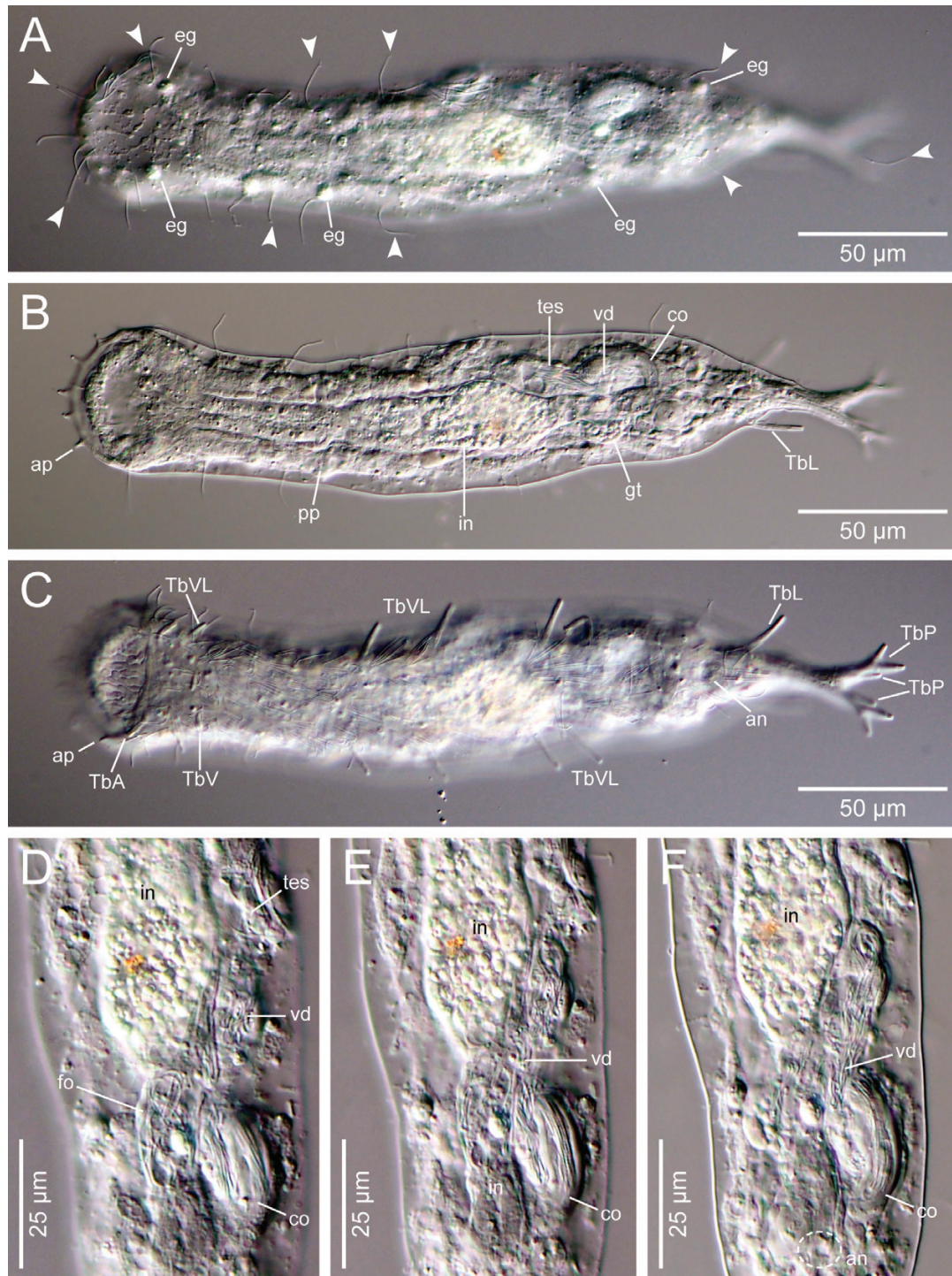
Figure 1. *Chimaeradasys oligotubulatus.* Schematic drawings of the holotype specimen. A, combined dorsal and internal view. B, ventral view. Abbreviations: ap, anterior papillae; co, caudal organ; eg, epidermal glands; fo, frontal organ; in, intestine; pp, pharyngeal pores; sci, sensory cilia; TbA/TbL/TbP/TbV/TbVL, anterior/lateral/posterior/ventral/ventrolateral adhesive tubes; te, testis.

Type specimen: The single specimen that was documented microscopically and described herein is the holotype, fixed by monotypy (Article 73.1.2. of the International Code of Zoological Nomenclature, ICZN, 1999). The holotype specimen does not exist any longer (Article 73.1.4. of the International Code of Zoological Nomenclature, ICZN, 1999). Declarations according to recommendations 73G–73J (ICZN, 2017): the living, anaesthetized specimen was extensively investigated microscopically in

order to gain optimal, taxonomy-relevant data. The morphological distinctness and uniqueness is the reason for naming this new taxon now. The specimen was recovered from the microscopic slide and immediately dissolved in order to extract genomic DNA for genetic analyses. The remaining genomic DNA was stored at –20 °C. None of the remaining sediment samples yielded further specimens of the new species. Several gastrotrich taxonomists have been consulted prior to this taxonomic act. The

Figure 2. *Chimaeradasys oligotubulatus*. Light microscopic images of the holotype specimen, differential interference contrast (DIC). A–C, habitus in dorsal, horizontal and ventral views. D–F, testes and accessory reproductive organs in different focal planes. Note the spermatozoa inside the frontal organ (D) and corkscrew-like sperm heads (E, F). Abbreviations: arrowheads, sensory cilia; an, anus; ap, anterior papillae; co, caudal organ; eg, epidermal glands; fo, frontat organ; gt, glandular tissue; in, intestine; pp, pharyngeal pore; TbA/TbL/TbP/TbV/TbVL, anterior/lateral/posterior/ventral/ventrolateral adhesive tubes; tes, testis; vd, vas deferens.

following recommendations regarding taxonomic processing of soft-bodied meiofauna (Garraffoni *et al.*, 2019) were applied: the specimen was observed and documented using high-resolution objectives and differential interference contrast (DIC), series of high-resolution digital images and a video sequence were deposited in MorphDBase (https://www.morphdbase.de/?A_Kieneke_20200503-S-1.1 respectively https://doi.org/10.20363/mdb.2w1k-mr22 and https://www.morphdbase.de/?A_Kieneke_20200501-M-70.1 respectively https://doi.org/10.20363/mdb.rj1d-8y15). The partial nuclear 18S rDNA and mitochondrial *COI* sequences have been deposited in the European Nucleotide Archive (ENA) at EMBL-EBI under accession number PRJEB38727 (https://www.ebi.ac.uk/ena/browser/view/PRJEB38727). The individual accession numbers are LR862428 (18S) and LR862427 (*COI*).

Material examined: Only the single holotype specimen was surveyed using light microscopy with DIC. Furthermore, the genomic DNA was extracted from the single specimen and used as a template for amplification of nuclear and mitochondrial gene fragments.

Ecology: Sediment was made up of fine, organogenous sand (granulometric data not available). Temperature, salinity, oxygen content and irradiation (photosynthetically active radiation from 400–700 nm) of the bottom water at the time of sampling were 14.5 °C/35.93 PSU/218 µmol/kg/160 µmol photons/m² and s, respectively (measured at a depth of 250 m during CTD deployment #77-1 of expedition M150 at 39°19,650'N, 031°16,430'W).

Diagnosis: A *Chimaeradasys* of 277 µm in total length and 50 µm in maximum width. Anterior adhesive tubes, one per side, in a row just posterior to the mouth; TbV, a single pair in the anterior pharyngeal region at U15; TbL, one per side at U85; TbVL, five per side, one of which was in the anterior pharyngeal region at U14 and the other four were unevenly distributed along the anterior half of the trunk; TbP, three per side, two at the end of each peduncular branch and one medial, inserting ventrally near the base of the branch. Mouth wide (up to 55 µm in breadth), leading to a shallow, funnel-shaped buccal cavity and surmounted dorsally by a scalloped oral hood. Pharynx 67 µm in length, with pores at U33; PhIJ at U34. Intestine straight, slightly wider at midbody; anal opening at U80. Hermaphrodites, single testis on right body side, beginning well posterior to the PhIJ at U43; caudal organ glandomuscular; frontal organ sac-like, both with spermatozoa inside; ovary and oocytes not seen.

Etymology: The species epithet is composed of the Greek ολιγος, little, and Latin *tubulus*, a small tube or hose, referring to the low number of ventrolateral adhesive tubes.

Description: The body measures 277 µm in total length (Figs 1A, B, 2A–C). The habitus shows a clear widening in the region of the mouth opening (U10) that is surmounted by a scalloped oral hood. The mouth measures 43 µm in diameter and continues in a shallow, funnel-shaped buccal cavity (Figs 1B, 2B, C). The region of the pharynx (U10 to U34) is slightly narrowed followed by the slightly widened trunk until approximately U55. The rear trunk continuously narrows until U87 and between U87 and U97, it is just a narrow peduncle that splits into a pair of short appendages (peduncular branches) at U97 (Figs 1A, B, 2B). Body width is 50/36/50/41/30/18/8 µm at U10/20/55/70/80/85/95, respectively. The trunk is dorsoventrally flattened with a flat venter and a moderately arched dorsum.

The adhesive tubes occur as anterior (TbA), ventral (TbV), lateral (TbL), ventrolateral (TbVL) and posterior (TbP) groups (Figs 1B, 2B, C). There is only a single pair of TbA. At U10, these two ventral TbA are placed close to the ventral (posterior) mouth rim (Figs 1B, 2C). The distance between the insertions of both tubes is 26 µm. Each TbA is about 7.5 µm long. At U15, a single pair of TbV is placed midventrally (Figs 1B, 2C). Each of the two TbV is about 5.5 µm long and the distance between both tubes is 13.5 µm. A single pair of TbL inserts at U85 (Figs 1A, 2B, C); TbL are about 18 µm long and project more posteriorly than laterally at an angle of less than 40° against the longitudinal axis of the animal. It has to be stressed that this single pair of TbL could, in principle, alternatively be defined as a fourth pair of TbP (see 'Taxonomic affinities'). There are five pairs of TbVL: the first pair inserts in the anterior pharyngeal region at U14, while the others are unevenly distributed from about the pharyngeo-intestinal region to about half the trunk at U37, U46, U59 and U62, respectively (Figs 1B, 2C). The most anterior TbVL are just 7.5 µm long, followed by the second pair with up to 12.5-µm long tubes, while all other TbVL measure between 16 and 18 µm in length. All TbVL project laterally and slightly towards posterior at an angle between 48° and 60° against the longitudinal axis of the animal. In total, there are six bilaterally arranged TbP, all confined to the peduncular branches (Figs 1B, 2C). In fact, each peduncular branch bears two tubes at its apex, arranged in a V-shaped manner, and a third tube along the medial margin, inserting ventrally near the base. Distal tubes measure 8.5 µm in length, while the proximal tube is 10.5 µm long. The ventral locomotory cilia start at U12 shortly posterior to the

ventral mouth rim and end posterior to the anus at about U85. In the pharyngeal region, the cilia cover the entire ventral surface and are weakly arranged in transverse rows. At about U40, locomotory cilia seem to split into two separated fields, each *c*. 10 µm in width and 20 µm spaced from each other at U50. Around U60, both fields fuse again and form a more or less uniform field of more sparsely placed cilia (Figs 1B, 2C). Length of ventral locomotor cilia varies between 11 and 14 µm. At least ten presumptively sensory cilia, up to 20 µm long, insert on the dorsal surface of the oral hood, roughly arranged in pairs. Further putative sensory cilia insert dorsolaterally along the trunk, arranged roughly pairwise (Figs 1A, 2A). Some of these cilia are associated with epidermal glands. Along the dorsal (anterior) and lateral parts of the mouth rim, there are seven evenly spaced and presumptively sensory papillae, each one measures about 4µm in height (Figs 1A, B, 2B). No cilia where directly linked to the papillae.

The holotype specimen had five pairs of bilaterally arranged epidermal glands at U10/22/30/64/79, respectively (Figs 1A, 2A). The globular to slightly pear-shaped glands had a diameter of 5 to 6 µm and appear with granular content. At least for the second and third pair, we were able to observe putative sensory cilia associated with the epidermal glands. In the area of the trunk, between roughly U33 and U62, glands seemed to be missing.

The digestive system starts anteriorly with the ample mouth opening that continues in a funnel-shaped buccal cavity. Fold-like structures at the dorsal epithelium of the buccal cavity and along the lip-like mouth rim indicate a certain contractile property of the whole oral basket (Figs 1B, 2C). The pharynx is about 67 µm in length with pharyngeal pores that open ventrolaterally at U31. The width of the musculoglandular pharynx is 42/16/11/14/22/11 µm at U10/15/20/25/31/33, respectively. The pharyngeo-intestinal junction is at U34 (Figs 1A, 2B). The intestine spans from U34 to U80, where it opens externally with an inconspicuous ventral anus (Fig. 2C, F). It has a maximum width in its middle-third and tapers considerably toward the anus. Widths are 16/19/22/12/8/5 µm at U35/45/55/60/70/75, respectively. Only a slight regionalization of the intestine is recognizable with a higher density of presumptively enzymatic vesicles in the middle-third and bigger, vacuole-like digestive vesicles in the posterior-third (Fig. 2B). The nature of the gut content was not ascertainable.

There is a single, 80-µm long right testis spanning from U43 to U73, including the posteriorly directed vas deferens (Figs 1A, 2B, D–F). However, since the actual termination of the sperm duct could not be determined with certainty (see below), the length measurement is just an approximation. The maximum width of the single testis is 15 µm at U60. Lateral to the posterior testis, between U62 and U76, there is a thick-walled, muscular hollow structure, presumptively the caudal organ (Figs 1A, 2B, D–F). It is roughly club-shaped and narrows posteriorly (maximum width is about 11 µm at the muscular section) into a kind of outlet duct that passes the intestine ventrally and forms a slight 'swelling' (9.5 µm in diameter) on the left side of the posterior intestine (Fig. 2D–F). Dorsal to the intestine, between U60 and U68 in a median position, there is a sac-like, 23 by 11 µm structure, the frontal organ (Fig. 2D). All three reproductive structures, testis, frontal and caudal organs, are filled with filiform spermatozoa with clearly spiralled sperm heads (Fig. 2D–F). While sperm lies in more or less parallel bundles inside the testis and the caudal organ, they are curled inside the frontal organ.

Remarks on external anatomy and reproductive structures: The apparent absence of maturing oocytes in the studied specimen of *Chimaeradasys oligotubulatus* is a likely indication that the specimen has not reached full adulthood. While we acknowledge that fully mature specimens may reach a larger size and may develop some additional adhesive tubes of the anterior and ventrolateral series, the well-formed spermatozoa inside the testis and caudal organ, and the motile spermatozoa inside the frontal organ, indicate that the size of fully grown adults will not be much different from that of the studied specimen. Likewise, the number of adhesive tubes will not undergo ample variations.

Furthermore, the studied specimen of *C. oligotubulatus* shows a heterogeneous organization of the ventral locomotory ciliation, i.e. cilia are organized in transverse bands in the anterior and posterior body regions, but as paired longitudinal bands at mid-trunk. Such an inhomogeneous organization is so far unreported among Gastrotricha. Considering that in *C. polytubulatus* (see below) the locomotory cilia are organized in transverse rows all over the ventral surface, we think the unusual organization of locomotor cilia observed in *C. oligotubulatus* represents an artefact rather than the natural condition, probably due to excessive compression of the specimen. Consequently, *C. oligotubulatus* should be considered to possess ventral cilia distributed in transverse rows that cover the entire ventral surface.

There are some uncertainties concerning the reproductive system of the new species. We were not able to unambiguously detect external and/or internal pores of either the testis, or the frontal and caudal organs. Furthermore, the connectivity between the three organs could not be clarified with certainty. If the function of these organs matches those of the

closest phylogenetically allied species (see below), as the incomplete information we currently have seems to suggest, most likely the vas deferens and the caudal organ open independently on the ventral side each with its own pore or via the anus (for a summary see, for example: Ruppert & Shaw, 1977; Ruppert, 1978; Kieneke & Schmidt-Rhaesa, 2015). Likewise, a direct internal connection between frontal and caudal organ (see: Ruppert, 1978; Kieneke *et al.*, 2009) is possible, but could not be demonstrated unequivocally. Neither a large egg nor any developing oocytes were observed in the single specimen of the new species. On the left side of the intestine, more or less in the same region as the frontal organ (between U60 and U72), there is an accumulation of droplets and globular material of presumptively glandular property, about 7 µm wide at U65 (Fig. 2B). We were not able to definitely clarify whether this is just vesicular mesodermal tissue or secretory material of an as yet undescribed gland.

Variability and remarks: Information on character variability among individuals of the new species is currently not available.

Taxonomic affinities: The taxonomic affinities of the new genus and both new species are discussed collectively below, following the description of the second new species.

CHIMAERADASYS POLYTUBULATUS SP. NOV.

(FIGS 3, 4)

Zoobank registration: urn:lsid:zoobank.org:act: DD1807A1-ED8C-4D76-9BE6-435BAFAAC278

Type locality: Italy, Sardinia, Costa Paradiso (41°3'8.84"N, 8°56'15.71"E); collection made on 4 September 2010 by scuba-diving at 35 m depth.

Type specimen: The single specimen that was documented microscopically and described herein is the holotype, fixed by monotypy (Article 73.1.2. of the International Code of Zoological Nomenclature, ICZN, 1999). The holotype specimen does not exist any longer (Article 73.1.4. of the International Code of Zoological Nomenclature, ICZN, 1999). Declarations according to recommendations 73G–73J (ICZN, 2017): the living, anaesthetized specimen was extensively investigated microscopically in order to gain optimal, taxonomy-relevant data. The morphological distinctness and uniqueness is the reason for naming this new taxon now. The specimen was recovered from the microscopic slide and stored in pure ethanol until dissolving it in order to extract genomic DNA for genetic analyses. The remaining genomic DNA was stored at –20 °C. None of the remaining sediment samples

yielded further specimens of the new species. Several gastrotrich taxonomists have been consulted prior to this taxonomic act. Following recommendations regarding taxonomic processing of soft-bodied meiofauna (Garraffoni *et al.*, 2019) were applied: the specimen was observed and documented using high-resolution objectives and DIC, series of high-resolution digital images were deposited in MorphDBase (https://www.morphdbase.de/?A_Kieneke_20200503-S-2.1 respectively https://doi.org/10.20363/mdb.mjky-s935).

Material examined: Only the single holotype specimen was surveyed using light microscopy with DIC. Furthermore, the genomic DNA was extracted from the single specimen and used as template for amplification of nuclear, as well as mitochondrial, gene fragments, although amplification has failed so far.

Ecology: Sediment was made up of coarse, well-sorted sand (mean grain size = –0.02 phi, sorting = 0.48). Temperature and salinity of the pore water at the time of tha samplings were 13 °C and 38 PSU, respectively.

Diagnosis: A *Chimaeradasys* of 391 µm in total length and 74 µm in maximum width. Anterior adhesive tubes, two per side, in a row just posterior to the mouth; TbV and TbD, absent; TbL, one per side at U86; TbVL, ten on the left side and 12 on the right side; the first tube of each side in the anterior pharyngeal region at U13 and the others unevenly distributed along the anterior two-thirds of the trunk; TbP, three per side, two at the end of each peduncular branch and one along the medial side, inserting ventrally near to the others. Mouth wide, (up to 60 µm in breadth), leading to a shallow, funnel-shaped buccal cavity and surmounted dorsally by a scalloped oral hood. Pharynx 92 µm in length, with pores at U28; PhIJ at U32. Intestine straight, slightly wider at midbody; anal opening at U78. Hermaphrodites; single testis on right body side, beginning just posterior to the PhIJ at U34; caudal organ glandomuscular; frontal organ sack-like, both with spermatozoa inside; ovary unpaired, large egg dorsal to intestine centered at U51.

Etymology: The species epithet is derived from Greek ϖολύ, much, and Latin *tubulus*, tubule, referring to the high number of ventrolateral adhesive tubes.

Description: The body measures 391 µm in total length (Figs 3A, B, 4A, B). The habitus shows a clear widening in the region of the mouth opening (U0 to U8) that is surmounted by a scalloped oral hood and an expanded mouth rim. The mouth measures 60 µm in diameter (Figs 3B, 4B, C). The region of the pharynx (U8 to U32) is slightly narrowed followed by

the slightly widened trunk until approximately U52. The rear trunk continuously narrows until U89 and, between U89 and U96, it is just a narrow peduncle that splits into a pair of short appendages at U96 (Figs 3A, B, 4A). Body width is 61/50/49/74/60/46/30/11 µm at U5/10/20/52/70/80/85/90, respectively. The trunk is dorsoventrally flattened with a flat venter and a moderately arched dorsum.

The adhesive tubes occur as anterior (TbA), lateral (TbL), ventrolateral (TbVL) and posterior (TbP) groups
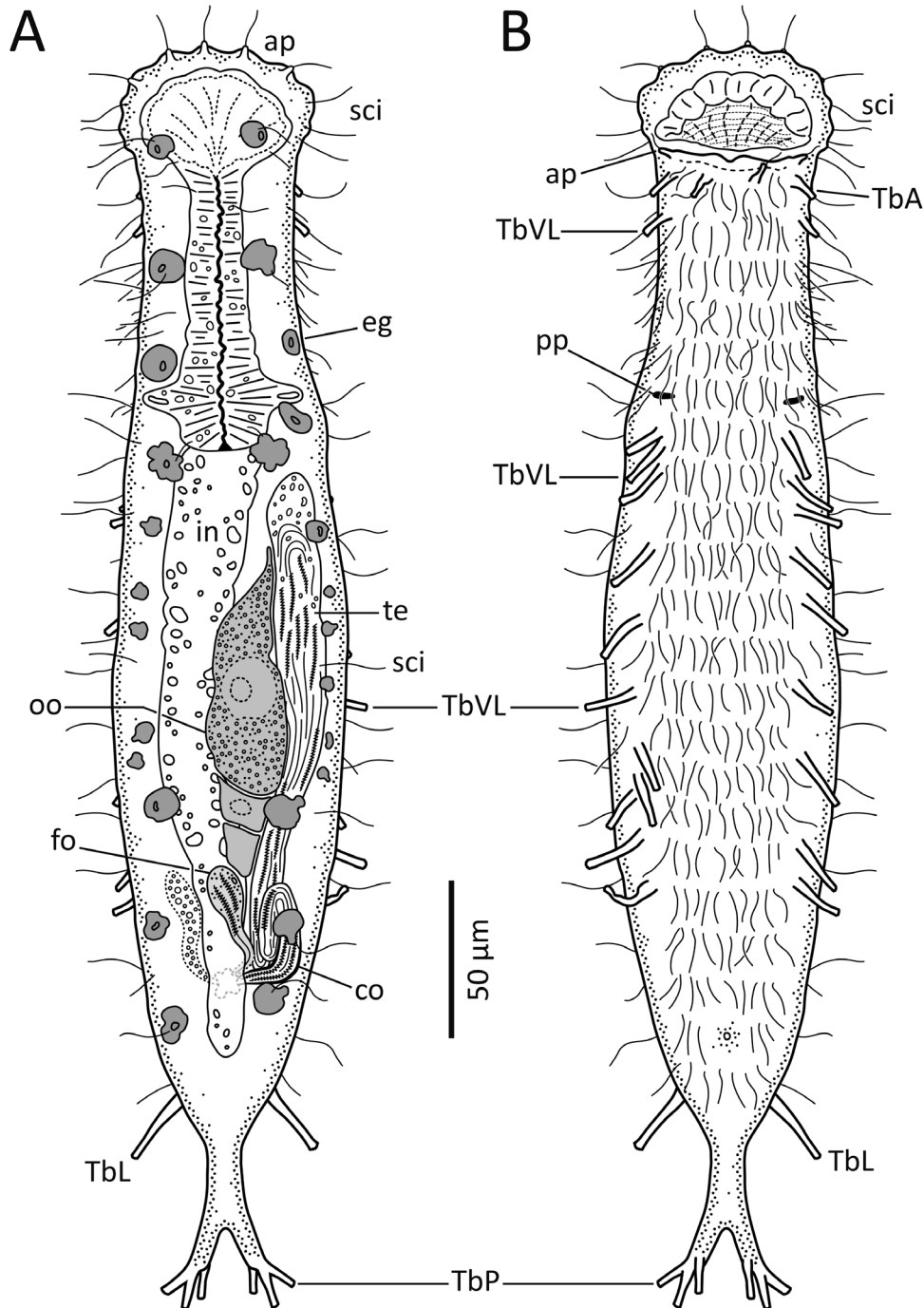
Figure 3. *Chimaeradasys polytubulatus*. Schematic drawings of the holotype specimen. A, combined dorsal and internal views. B, ventral view. Abbreviations: ap, anterior papillae; co, caudal organ; eg, epidermal glands; fo, frontal organ; in, intestine; oo, mature oocyte; pp, pharyngeal pores; sci, sensory cilia; TbA/TbL/TbP/TbVL, anterior/lateral/posterior/ventrolateral adhesive tubes; te, testis.
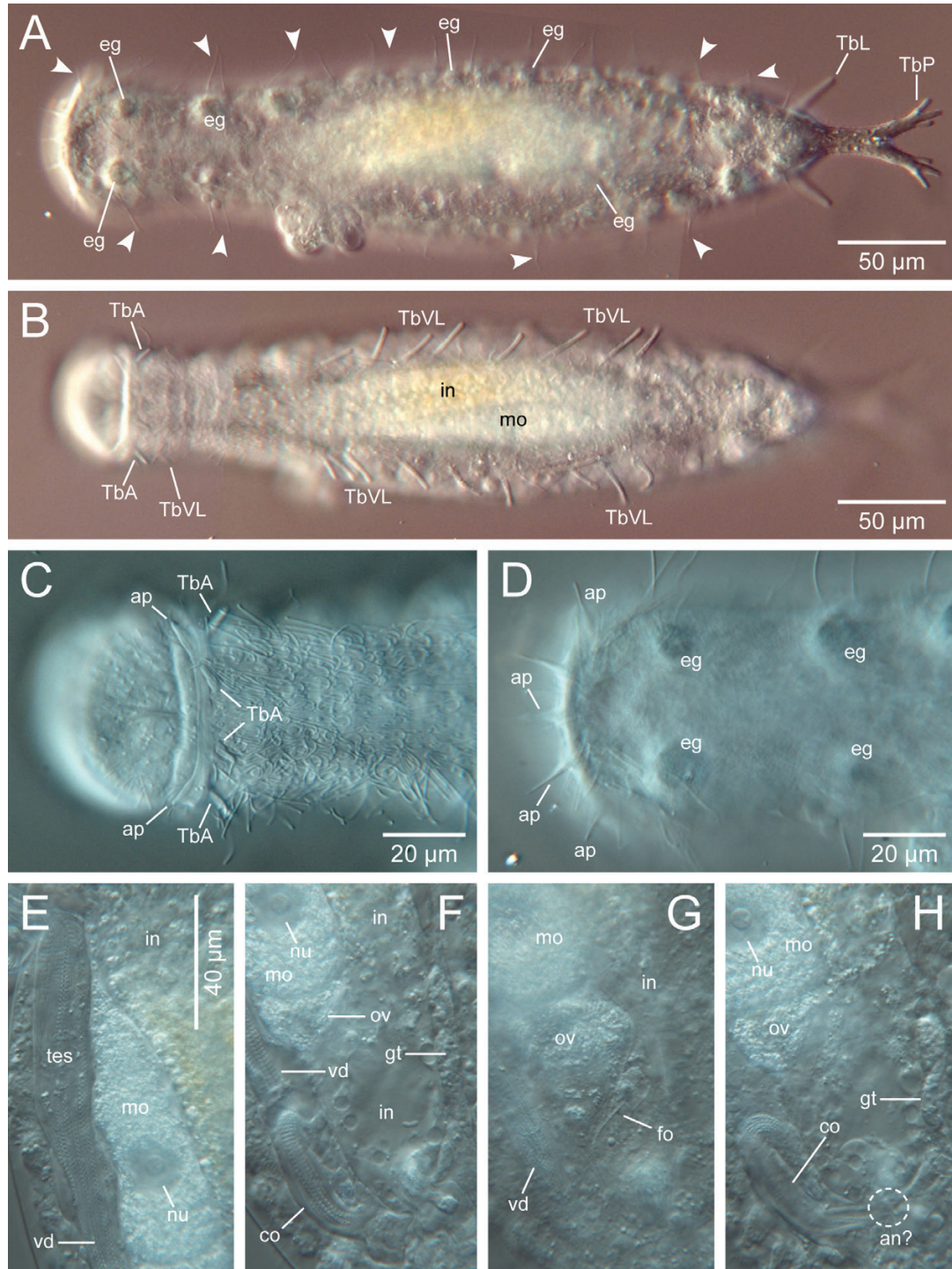
Figure 4. *Chimaeradasys polytubulatus*. Light microscopic images of the holotype specimen, DIC. A, B, habitus in dorsal and ventral views. C, D, anterior end in ventral and dorsal views. E–H, gonads and accessory reproductive organs in different focal planes. Note the corkscrew-like sperm heads (E, F) and spermatozoa inside the frontal organ close to the ovary (G). Abbreviations: arrowheads, sensory cilia; an, anus; ap, anterior papillae; co, caudal organ; eg, epidermal glands; fo, frontat organ; gt, glandular tissue; in, intestine; mo, mature oocyte; nu, nucleus of mature egg; ov, ovary; TbA/TbL/TbP/TbVL, anterior/lateral/posterior/ventrolateral adhesive tubes; tes, testis; vd, vas deferens.

(Figs 3A, B, 4A–C). There are two pairs of TbA. At U11, these two pairs of TbA are placed close to the ventral (posterior) mouth rim. Especially the inner pair may be masked by the withdrawn ventral, lip-like mouth rim (Figs 3B, 4C). The distance between the insertions of both inner tubes is 16 µm and between the outer TbA it is 39 µm. The outer TbA are about 9 µm long, while the inner TbA are shorter (6–7 µm) and much more delicate. A single pair of TbL inserts at U86 (Figs 3A, B, 4A); TbL are about 23 µm long and project laterally and towards posterior at an angle of 38° against the longitudinal axis of the animal. The TbVL occur in different numbers on left and right sides, mostly in the middle-third of the body (Figs 3B, 4B). In total, there are ten pairs of TbVL inserting at U14, between U32 and U37, at U41, U46, U52, U58, U65 and U68, respectively. The most anterior TbVL are just 8–9 µm long, while all other TbVL measure between 15 and 19 µm in length. All TbVL project laterally and towards the posterior at an angle between 29° and 55° against the longitudinal axis of the animal. In addition to these paired TbVL, the examined specimen shows two further tubes on the right side, between U59 and U61. In total, there are six bilaterally arranged TbP, all confined to the peduncular branches (Figs 3B, 4A). Each branch shows two tubes at the distal end, arranged in a V-shaped manner, and a third tube along the medial margin, inserting ventrally near the other two tubes. Distal tubes measure 10 µm in length, the medial tube is 12 µm long.

The ventral locomotory cilia start at U10 shortly posterior to the ventral mouth rim and end posterior to the anus at about U85. The cilia cover the entire ventral surface and are distinctly arranged in transverse rows (Figs 3B, 4C). The field of locomotor cilia has a more or less uniform width of about 42 µm, but the density of cilia decreases slightly towards the posterior. Length of ventral locomotor cilia varies between 10 and 15 µm. At least four presumptively sensory, up to 12 µm long and pairwise arranged cilia insert on the dorsal surface of the oral hood. Further putative sensory cilia insert dorsolaterally along the trunk, arranged roughly pairwise (Figs 3A, 4A, D). Some of these cilia are associated with epidermal glands. Along the dorsal (anterior) and lateral parts of the lip-like mouth rim, there are 13 presumptively sensory papillae, each one measures about 4 µm in height (Figs 3A, B, 4C, D). The seven most anterior sensory papillae are evenly spaced from each other, while the distance between papillae decreases towards the lateral rims of the mouth opening. There is a *c*. 14-µm long cilium inserting on the tip of each papilla.

The surveyed specimen has seven pairs of more or less bilaterally arranged epidermal glands at about U8/18/25/33/62/71/79, respectively (Figs 3A, 4A, D). The irregular, globular or slightly pear-shaped glands have a diameter of 9 to 11 µm and appear with granular content. At least for some glands, we were able to observe putative associated sensory cilia. In the area of the trunk, between U35 and U60, there are further epidermal glands in a roughly pairwise arrangement. However, these glands are much smaller and measure just 4 to 6 µm in diameter. Regarding the epidermal gland system, there is a certain degree of asymmetry, i.e. there are also some unpaired glands.

The digestive tract starts anteriorly with the ample mouth opening that continues in a funnel-shaped buccal cavity. Fold-like structures at the dorsal epithelium of the buccal cavity and along the lip-like mouth rim indicate a certain contractile property of the whole oral hood (Figs 3B, 4C). The pharynx is 91 µm in length with pharyngeal pores that open ventrolaterally at U28. The pharyngeo-intestinal junction is at U32 (Fig. 3A). The width of the musculoglandular pharynx is 48/18/19/23/51/25 µm at U6/11/20/25/28/32, respectively. The intestine spans from U32 to U82, where it opens externally with an inconspicuous ventral anus. It has a more or less constant width of about 20 to 25 µm in its anterior half and tapers gradually toward the anus. Widths are 25/22/20/15/11 µm at U40/50/60/70/80, respectively. Only an inconspicuous regionalization of the intestine is recognizable with a higher density of refractive, presumptively enzymatic vesicles in the anterior two-thirds and bigger, vacuole-like digestive vesicles in the posterior-third (Fig. 4B). At low magnification, the middle-third of the intestine shows up in a greenish to brownish colour. However, the nature of the gut content was not ascertainable.

There is a single, 165-µm long right testis spanning from U35 to U76, including the posteriorly directed vas deferens that starts at about U60 (Figs 3A, 4F). However, the actual termination of the sperm duct could not be determined with certainty (see below). The maximum width of the single testis is 16 µm at U50. Apart from the most anterior portion that is filled with vesicular content (approximately U35 to U40), the whole testis, including the vas deferens, is stuffed with filiform spermatozoa with clearly spiralled sperm heads (Fig. 4F). Lateral to the posterior (distal) portion of the vas deferens, between U68 and U76, there is a thick-walled, muscular, hollow structure, presumptively the caudal organ (Figs 3A, 4F, H). It is roughly club-shaped and narrows posteriorly (maximum width is about 8 µm at the muscular section at U74) into a kind of outlet duct that curves to the left and ventrally under the intestine. The anterior (proximal) portion seems to be folded by almost 180° and reclines parallel and medial to the muscular section of the caudal organ (Figs 3A, 4F, H). Dorsal to the intestine in a median position, between U67 and U75, there is a sac-like structure measuring roughly 10 by 31 µm, the frontal organ (Figs 3A, 4G). In addition to

the testis, there are filiform spermatozoa with clearly spiralled heads inside the frontal and caudal organs (Fig. 4F–H). While sperm lies in dense, more or less parallel bundles inside the testis and the caudal organ, there are only few, single and coiled spermatozoa inside the frontal organ. Slightly dorsal and lateral to the right side of the intestine there is an unpaired ovary spanning between U40 and U67 (Figs 3A, 4B, E–H). Between approximately U60 and U67 there are a few early oocytes (10–20 µm in diameter) that mature in a cephalic direction. Between U40 and U60 there is a large, roughly drop-shaped egg (26 by 80 µm) densely filled with refractive vesicles and containing a large nucleus (almost 19 µm in diameter) with distinct nucleolus (Fig. 4E).

Remarks on external anatomy and reproductive structures: The observed specimen is characterized by an interesting asymmetry, which concerns the adhesive tubes of the ventrolateral series. More specifically, it shows ten TbVL on the left side and 12 TbVL on the right side. Phenomena of asymmetry regarding tubes of the ventral and ventrolateral series has previously been reported several times within marine Gastrotricha and appear to be particularly frequent in taxa of the subfamily Thaumastodermatinae, e.g. *Ptychostomella orientalis* Lee & Chang, 2003, *Tetranchyroderma inequitubulatus* Todaro, Balsamo & Tongiorgi, 2002 and *T. weissi* Todaro, 2002 (Todaro, 2002; Todaro *et al.*, 2002; Lee & Chang, 2003).

Similar to the specimen of *C. oligotubulatus*, this specimen also has some uncertainties concerning the three reproductive structures: testis, the frontal and the caudal organs. We were not able to unambiguously detect external and/or internal pores. However, the spermatozoa inside the frontal organ are in closest proximity to the mature or maturing egg, respectively. Furthermore, the connectivity between the three organs could not be clarified with certainty. But as in the other new species, our incomplete data indicate accordance of function of these reproductive organs with that of phylogenetically allied species of the taxon Thaumastodermatinae. Hence, the vas deferens and caudal organ much likely open independently on the ventral side or throughout the anus and there probably is a connection between the frontal and the caudal organ lumina. On the left side of the intestine, more or less in the same region as the frontal organ, around U70, there is an accumulation of droplets and globular material about 7 µm wide (Fig. 4F, H). We were not able to clarify whether this is just vesicular mesodermal tissue, or secretory material of a new type of gland.

Variability and remarks: Information on character variability among individuals of the new species is currently not available.

TAXONOMIC AFFINITIES

Based on general appearance, we initially regarded the discovered specimens either as belonging to *Dendrodasys* (fam. Dactylopodolidae), due to the branched caudal peduncle, or to the Thaumastodermatidae, perhaps close to *Ptychostomella* in virtue of the wide mouth and the bare cuticular covering. Undeniably, at first sight both new species appear like 'chimeras' of both mentioned genera, being 'compound' from the anterior two-thirds of a *Ptychostomella* and the posterior-third of a *Dendrodasys* (Fig. 5A–C).

The peculiar posterior body region, ending with the narrow peduncle that splits into two short appendages, whose tips are equipped with adhesive tubes, resembles the anatomic condition of *Dendrodasys* (see, for example, the recently described *D. rubomarinus* Hummon, 2011; see also Fig. 5A). The two noticeable and posteriorly directed lateral adhesive tubes shown by the new species amplify the overall similarity of their posterior body region with that of *Dendrodasys* because a pair of similar tubes is present also in members of the latter taxon (e.g. *D. duplus* Lee, 2012 and *D. gracilis* Wilke, 1954; see also Fig. 5A). However, there is an important difference regarding this character: while in *Dendrodasys* these tubes insert on the elongate posterior peduncle (less often at its base), in *Chimaeradasys* they are clearly inserted anterior to it. The situation concerning the gonads is somewhat ambiguous. In general, *Dendrodasys* possesses paired testes and paired ovaries (e.g. Wilke, 1954; Schmidt, 1974; Valbonesi & Luporini, 1984; Hummon, 2011), but at least one species, *Dendrodasys affinis* Wilke, 1954 (Fig. 5A) possesses a single right testis and a single ovary (see: Hummon *et al.*, 1998), therefore matching the new species concerning these characters. Another species, *D. duplus*, shows a certain reduction of the right testis (Lee, 2012) pointing to a phenomenon that is recurrent in Gastrotricha (e.g. in *Urodasys*; see: Schoepfer-Sterrer, 1974; Todaro *et al.*, 2019a). The reported instances indicate that reduction and/or complete loss of testes, respectively, in *Dendrodasys* happened at least twice independently, while such a character loss occurred only once within the stem lineage of the Thaumastodermatinae (Todaro *et al.*, 2011; Kieneke & Schmidt-Rhaesa, 2015). But there are even more striking dissimilarities between both new species and *Dendrodasys*: first, the anterior adhesive tubes of *Dendrodasys* (always a single pair) are borne on extensible fleshy bases; second, none of the hitherto known species of *Dendrodasys* possesses lateral or ventrolateral adhesive tubes (Fig. 5A); and, third, there are only two adhesive tubes per posterior appendage instead of three like in both new species of the new genus (Fig. 5A, B).
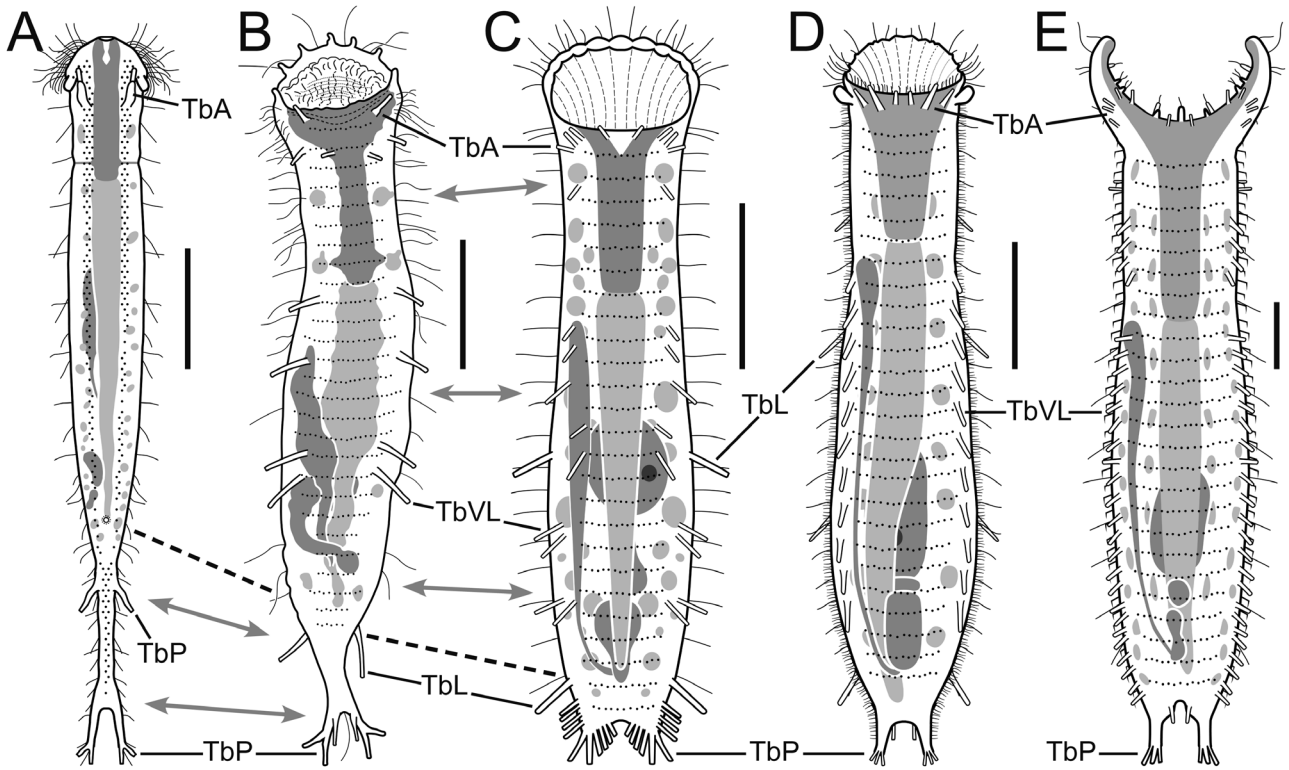
Figure 5. Comparison of genera related and non-related to *Chimaeradasys*. Schematic drawings show a combination of ventral views with internal structures. Intestinal, epidermal gland and reproductive systems (gonads, accessory organs) are displayed in greyscale. All scale bars 50 μm. A, *Dendrodasys affinis*. B, *Chimaeradasys oligotubulatus*. C, *Ptychostomella higginsi*. D, *Tetranchyroderma bronchostylus*. E, *Pseudostomella klauserae*. Dashed lines and double arrows indicate 'chimeric' composition of *Chimaeradasys*. Abbreviations: TbA/TbL/TbP/TbVL, anterior/lateral/posterior/ventrolateral adhesive tubes. A, C–E: modified from Kieneke *et al.* (2020).

Species of the new genus are also strikingly similar to members of Thaumastodermatidae Remane, 1927. Species of this family possess an ample mouth surmounted by an oral hood, which is diagnostic of the family. Importantly, the new species also share additional characteristics with members of the subfamily Thaumastodermatinae Remane, 1927, including the following: (1) anterior adhesive tubes originating directly from the body surface, (2) presence of ventrolateral adhesive tubes, (3) paired posterior 'adhesive pedicles', (4) small posterior pharyngeal pores, (5) unpaired right testis and (6) single ovary with gametes maturing in a caudocephalic direction (Fig. 5B–E; Ruppert, 1978; see also: Kieneke & Schmidt-Rhaesa, 2015). Among the Thaumastodermatinae, the new species are most comparable with species of *Ptychostomella* with which they share also the arrangement of the anterior adhesive tubes and the unarmored (bare/smooth) cuticle (Fig. 5B, C). However, due to the extremely exceptional shape of their posterior region, we regard both new species as part of an evolutionary lineage

distinct from that of *Ptychostomella*, supporting, therefore, the erection of a new genus that we name *Chimaeradasys* here. The results of the molecular phylogenetic analyses (see below) provide further support for this proposal.

Several morphological differences between the two discovered specimens support the idea of two species within the new genus. These are a smaller total body length, less anterior and ventrolateral adhesive tubes, less sensory papillae and a lower number of epidermal glands in *Chimaeradasys oligotubulatus* compared with *C. polytubulatus*. Furthermore, *C. oligotubulatus* possesses a pair of ventral adhesive tubes that are absent in *C. polytubulatus*. Also, the geographic distance between the two type localities may account for the erection of two new species. Of course, we cannot completely rule out that the aforementioned differences just represent the range of character variability of one widespread species, because we only were able to investigate a single specimen per location. However, the presence of two separate species, one occurring at the Azores and another at Sardinia, is

the most likely hypothesis that has to be tested once further data are available.

DISCUSSION

Chimaeradasys is morphologically unmistakable and distinctly diagnosable because of a unique combination of characters that makes it appear as a 'chimera' of two previously known genera. Furthermore, the obtained DNA sequences will enable future recognition of the new taxon, or even new species, based on sequence data. The results of our phylogenetic analyses are congruent with the findings of previous analyses based on the 18S ribosomal RNA gene (e.g. Todaro *et al.*, 2014, 2015, 2019b). The inclusion of the sequence of the new species confirms the overall scenario, especially regarding the monophyly of most genera of Macrodasyida and the families Thaumastodermatidae, Turbanellidae, Planodasyidae and Redudasyidae. Likewise, our results also challenge the monophyly of some traditional taxonomic units, such as the Cephalodasyidae and Macrodasyidae. The latter group congruently splits into a lineage comprising *Macrodasys*, *Thaidasys* Todaro, Dal Zotto & Leasi, 2015 and *Kryptodasys* Todaro, Dal Zotto, Kånneby, Hochberg, 2019, and a second lineage represented by species of *Urodasys* [compare Todaro *et al.* (2019b) with our trees based on the ML and BI analyses; Figs 6, 8]. A further conflict between traditional taxonomic classification and the results of molecular phylogenetic analyses is the possible non-monophyly of the genera *Tetranchyroderma* and *Ptychostomella*. While the latter group was resolved as a monophylum in earlier analyses (Todaro *et al.*, 2011), it was later resolved as paraphyletic (Todaro *et al.*, 2014, 2015, 2019b; present study). Such differences may be due to the different taxon sampling in the various studies, which was much higher in the work by Todaro *et al.* (2011) compared to the others. Regardless of the taxon sampling, *Tetranchyroderma* has always been recovered as non-monophyletic, which raised doubts about the characters currently used for the diagnosis of the genus. To be more precise, previous studies revealed *Tetranchyroderma* as two separate clades with *Ptychostomella*, or at least one of its included species, allied to one of these clades (Todaro *et al.*, 2011, 2014, 2015, 2019b). Such a scenario could be conceivable because there are species of *Tetranchyroderma* that show a reduced coverage of hooks, such as *Tetranchyroderma hypopsilancrum* Hummon, Todaro & Tongiorgi, 1993, *Tetranchyroderma anomalopsum* Hummon, Todaro, Balsamo & Tongiorgi, 1996 or *T. oligopentancrum* Hummon & Todaro, 2009 (see: Hummon *et al.*, 1993, 1996; Hummon &

Todaro, 2009). This might indicate a certain ancestral tendency towards 'nudity' of a clade covering these species plus species of *Ptychostomella* with their completely bare cuticle [see discussion of Todaro *et al.* (2011)]. The fact that certain species of *Ptychostomella* indeed possess cuticular differentiations, such as ventrolateral columns of slender papillae as, for instance, in *P. brachycephala* Lévi, 1954, lamellate scales in a comparable position in *P. lamelliphora* Todaro, 2013 or even a complete covering with almost circular ornaments in *P. lepidota* Clausen, 2000 (see: Clausen, 2000; Todaro, 2013) might further support such a scenario, since those structures could represent strongly modified remainders of the ancestral multipronged hooks. Such cuticular modifications up to complete absence of multi-ancres, as for instance in *Ptychostomella higginsi* Clausen, 2004 (see: Clausen, 2004), would definitely represent derived character states. On the other hand, the failure to recover the most species-rich and morphologically homogeneous macrodasyidan genus (*Tetranchyroderma* currently includes 87 species; WoRMS, 2020) as a monophyletic group may also be a hint that a different approach, such as phylogenomics, is needed. However, such a study is beyond the scope of the present paper and also not feasible with the scarce genetic material at hand (i.e. a single specimen of *C. oligotubulatus*).

Two of our analyses (ML and MP; Figs 6, 7) indicated *C. oligotubulatus* as sister-taxon to a clade containing species of *Pseudostomella*, *Ptychostomella* and *Tetranchyroderma*. By contrast, the BI analysis (Fig. 8) shows the new species allied with species of *Ptychostomella* and *Tetranchyroderma*, and revealed *Pseudostomella* as the sister-taxon of this clade. However, it is most important that, regardless of the slightly differing topologies (MP, ML or BI), the new species neither formed a supported sister-group relationship with any of the previously mentioned genera, nor with a member of the Dactylopodolidae, viz. sequences of *Dactylopodola*. In summary, this points (1) to the uniqueness of this animal as representative of a distinct phylogenetic lineage and (2) to its reliable affiliation to the Thaumastodermatinae. These issues, therefore, confirm our hypothesis of a new genus of this subfamily put forward on morphological data. Because our results do not fully resolve relationships among the most derived members of Thaumastodermatinae, different scenarios regarding the evolution of the multipronged hooks are conceivable. An affiliation of *Chimaeradasys* among *Tetranchyroderma* and *Ptychostomella* could indicate a secondary loss of multi-ancres, as already discussed above. If *Chimaeradasys* represents the sister-lineage of a clade consisting of *Pseudostomella*, *Ptychostomella* and *Tetranchyroderma* (see Figs 6, 7), a reduction and/or
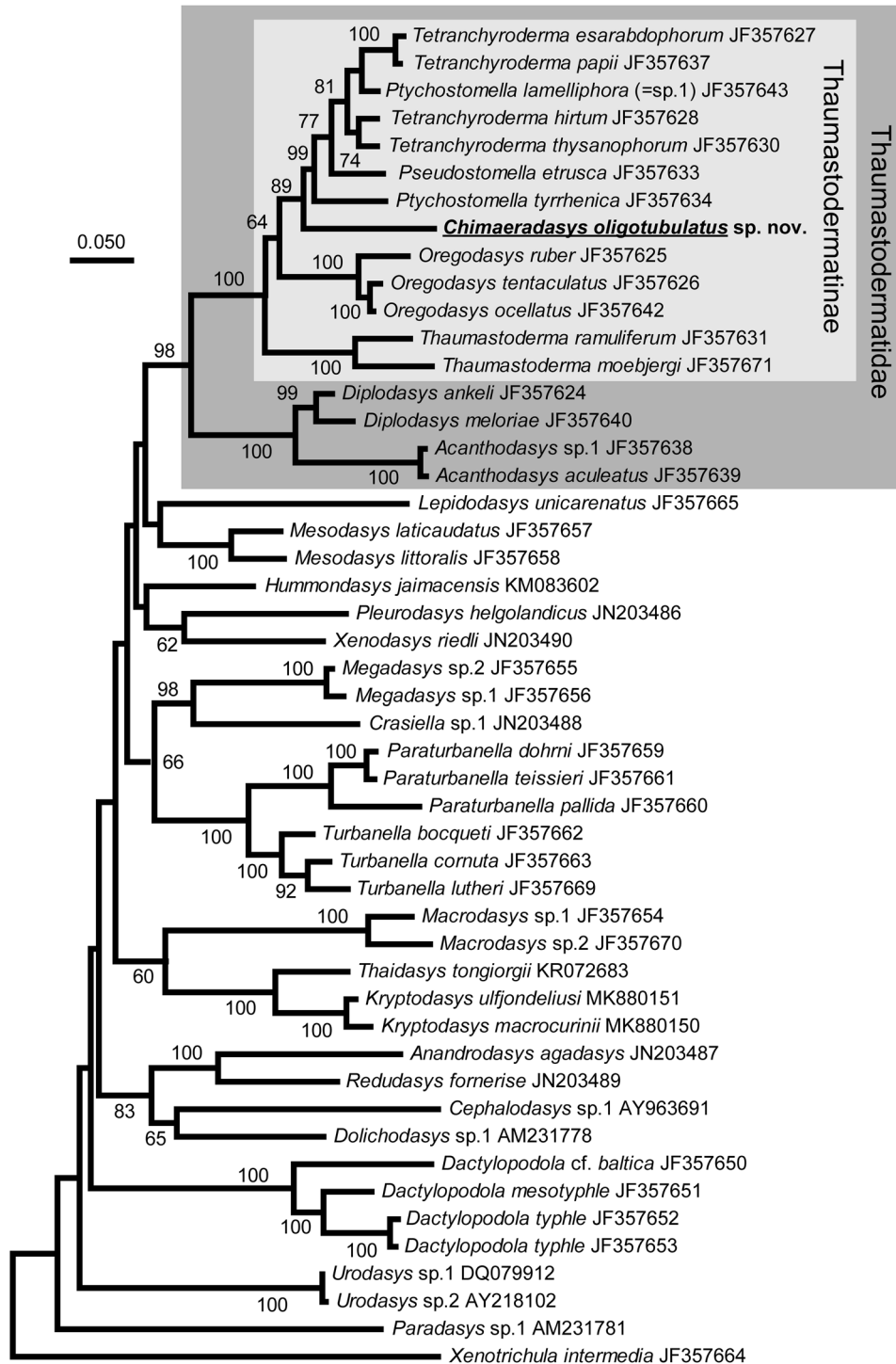
Figure 6. Phylogenetic relationships of the new genus and species *Chimaeradasys oligotubulatus* inferred from maximum likelihood analysis of a dataset of 18S rRNA-gene sequences. The analysis includes 49 sequences of 48 species of Macrodasyida and the outgroup is represented by the chaetonotidan *Xenotrichula intermedia* (Xenotrichulidae). The tree with the highest log-likelihood (-21098.83) is shown. The tree is drawn to scale, with branch lengths measured in the number of substitutions per site; the GTR+I+G model for nucleotide substitution was applied. Numbers at nodes represent bootstrap values (1000 replicates); only values > 60 are reported. Evolutionary analyses were conducted in MEGA X (Kumar *et al.*, 2018).
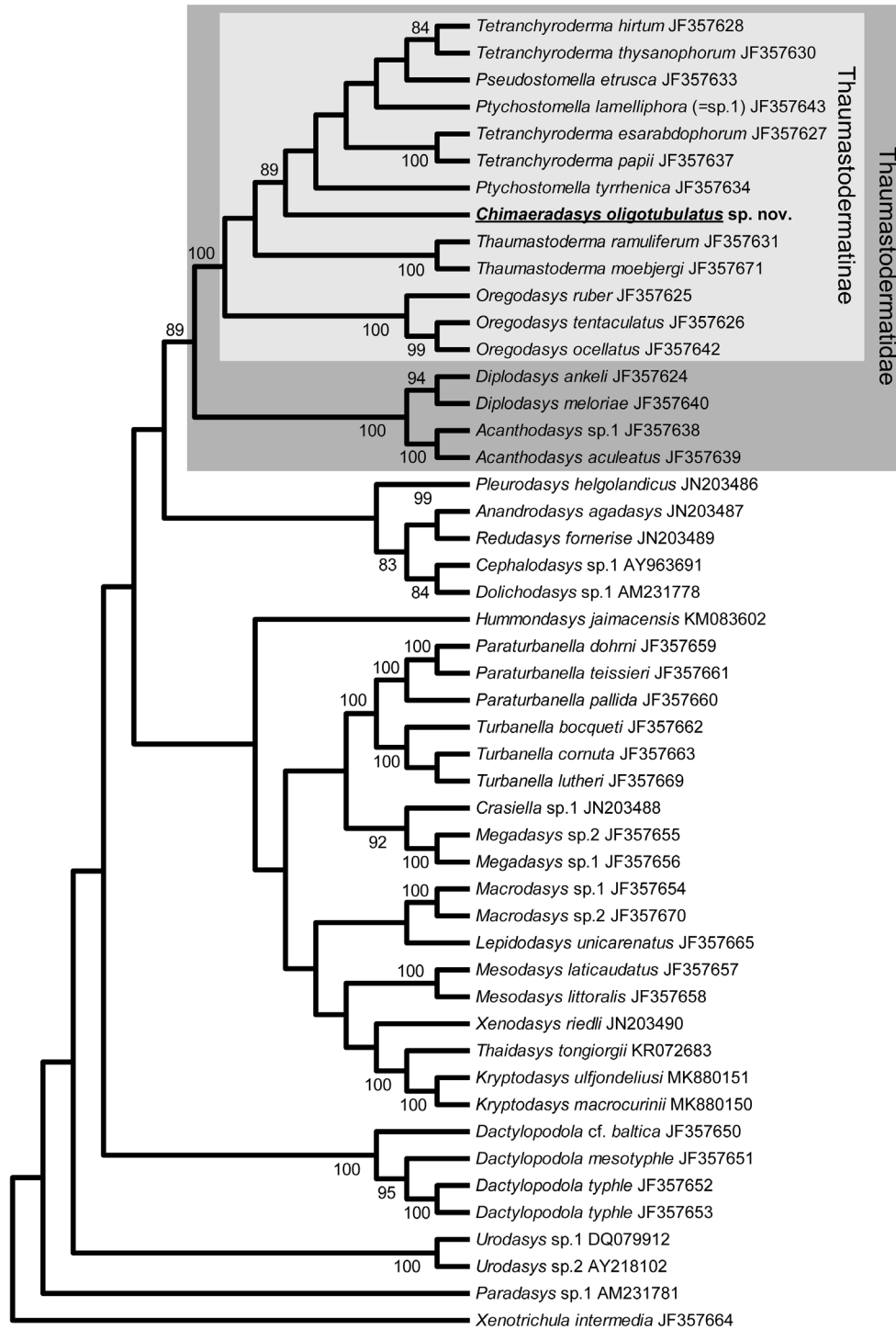
Figure 7. Phylogenetic relationships of the new genus and species *Chimaeradasys oligotubulatus* inferred from maximum parsimony analysis of a dataset of 18S rRNA-gene sequences. The analysis includes 49 sequences of 48 species of Macrodasyida and the outgroup is represented by the chaetonotidan *Xenotrichula intermedia* (family Xenotrichulidae). The most parsimonious tree with length = 4262 is shown. The consistency index is 0.352343, the retention index is 0.579185, and the composite index is 0.204072 (0.224227) for parsimony-informative sites (for all sites in parentheses). Numbers at nodes represent bootstrap values (1000 replicates); only values > 60 are reported. Evolutionary analyses were conducted in MEGA X (Kumar *et al.*, 2018).
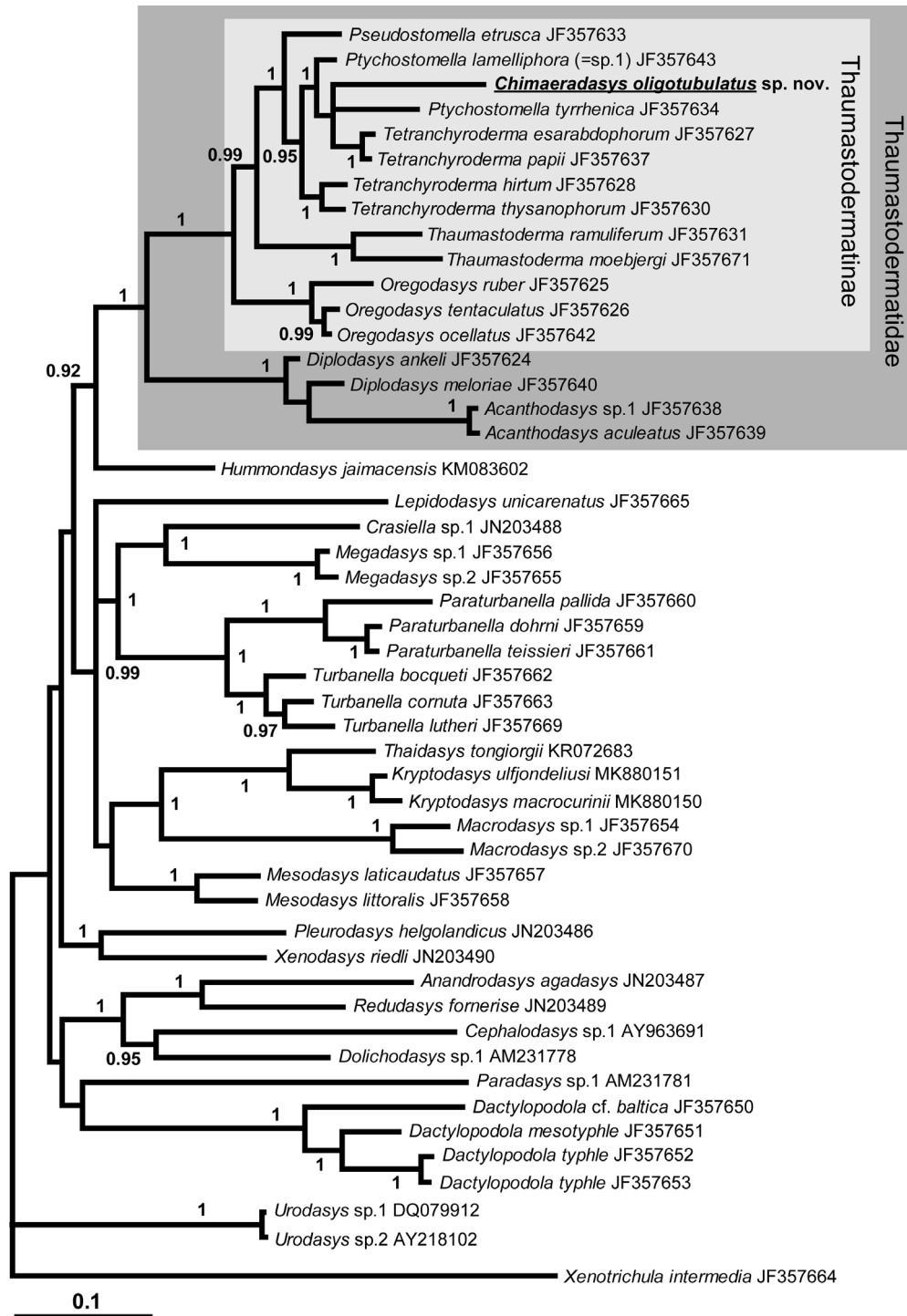
Figure 8. Consensus tree of 99 750 sampled trees from the Bayesian inference (BI) search on the 18S rRNA gene alignment of 49 gastrotrich sequences of 48 species using the GTR+I+G model for nucleotide substitution. Averaged branch lengths are proportional to substitutions per site under the used model. Bayesian posterior probabilities are provided next to branches or corresponding nodes, respectively.

loss of cuticular armature at least twice independently is most parsimonious. In this context, a possible most basal position of the 'spineless genus' *Oregodasys* within Thaumastodermatinae has to be considered too (see: Todaro *et al.*, 2014, 2015).

The analysis of the *COI* dataset yielded only weak resolution among the basal splits, which sometimes led to paraphyly of genera (see Supporting Information, Fig. S1). In general, phylogenetic performance of the *COI* gene is arguable due to high-rate heterogeneity in all of the cytochrome oxidase genes (Mueller, 2006). However, since the *COI* gene is considered as the most important barcoding gene for metazoans (Bucklin *et al.*, 2011; Hebert *et al.*, 2003; but see concerns in: Mueller, 2006), the sequence of *Chimaeradasys oligotubulatus* will certainly be of high value as a reference sequence for any future biodiversity assessment using barcoding (Bucklin *et al.*, 2011) or metabarcoding techniques (Bleidorn, 2017). The overall robust clustering and support of species resulting from our analysis might be taken as indication for a good suitability of the mitochondrial *COI* gene as a barcode for Macrodasyida. Such a 'qualification' was demonstrated for freshwater species of Paucitubulatina, as well (Kånneby *et al.*, 2012). However, it has to be stressed that we are not able to estimate inter- vs. intraspecific genetic variation, which is crucial for unambiguous barcoding approaches (Bucklin *et al.*, 2011).

The current study of gastrotrichs from the Azores and Sardinia is part of a larger pattern of independent studies that aim to solve the meiofauna paradox, i.e. that microscopic metazoa can have widespread geographic distributions in the absence of dispersal stages (e.g. Giere, 2009; Cerca *et al.*, 2018). The research programme during which *C. polytubulatus* was found tackled the issue by focusing on meiofauna from the littoral and shallow sublittoral fauna of two distinct geographic areas: the western coast of Sweden and the north-western coast of Sardinia. Partial results of this research may be found in Curini-Galletti *et al.* (2012); a follow-up study that includes also the island of Lanzarote (Canary Islands, Spain) may be found in Martínez *et al.* (2019). The larger project that led to the discovery of *C. oligotubulatus* concentrates on seamounts and oceanic islands, and examination of data is still running. George (2013) reviewed the potential role of seamount summits either as stepping-stones/staging-posts (see: MacArthur & Wilson, 1967) for a successive dispersal of shallow-water interstitial meiofaunal species over long distances or, alternatively, as a kind of 'collecting basin' of accidentally stranded individuals that subsequently establish new subpopulations. The latter might undergo isolated evolution, which could lead to local endemism or even adaptive radiation (George, 2013). Examples for both scenarios could be demonstrated for

the harpacticoid Copepoda (e.g. George & Schminke, 2002; George, 2004; Koller & George, 2011; and further studies summarized by: George, 2013). Initial studies on Gastrotricha from seamounts also seem to indicate both a stepping-stone function evidenced by the occurrence of several widespread species and a 'trap function' indicated by some local endemic taxa (Clausen, 2004; George, 2013). Although supposed endemism might be an artefact biased by insufficient research (George, 2013), it is nevertheless noticeable that peculiar new forms of marine gastrotrichs, such as *Hummondasys jamaicensis* Todaro, Leasi & Hochberg, 2014, *Urodasys completus* Todaro, Cesaretti & Dal Zotto, 2017 or *Chimaeradasys*, were discovered in geographically isolated island biotopes (Todaro *et al.*, 2014, 2019c; present study).

CONCLUSIONS

Our combination of morphological information with the analysis of DNA sequence data fulfils certain demands for an integrative taxonomy (Dayrat, 2005), although we are unable to present any information on intraspecific variation of both new species, neither morphologically nor genetically. We agree with George & Plum (2009) that species descriptions are indeed testable hypotheses, even if based on a single specimen only. If additional material (either specimens, sequences or both) become available in the future, any such hypothesis might get further support, or can, alternatively, be falsified. The integration of both data types (morphology and DNA sequences) enabled an extensive description of the new taxa (a new genus with two new species) and a reliable integration into the current phylogenetic systematization of the superordinated phylum, the Gastrotricha. The fact that both new species are so far only reported from remote island biotopes may be taken as evidence for an isolated evolution in such oceanic ecosystems.

REFERENCES

Blanco-Berical L, **Bradford-Grieve J**, **Bucklin A. 2011.** Molecular phylogeny of the Calanoida (Crustacea: Copepoda). *Molecular Phylogenetics and Evolution* **59:** 103–113.

Bleidorn C. 2017. *Phylogenomics. An introduction.* Heidelberg: Springer Nature.

Bucklin A, **Steinke D**, **Blanco-Berical L. 2011.** DNA barcoding of marine metazoa. *Annual Review of Marine Science* **3:** 471–508.

Cerca J, **Purschke G**, **Struck TH. 2018.** Marine connectivity dynamics: clarifying cosmopolitan distributions of marine interstitial invertebrates and the meiofauna paradox. *Marine Biology* **165:** 123.

Clausen C. 2004. Gastrotricha from the Faroe Bank. *Sarsia* **89:** 423–458.

Curini-Galletti M, **Artois T**, **Delogu V**, **De Smet WH**, **Fontaneto D**, **Jondelius U**, **Leasi F**, **Martínez A**, **Meyer-Wachsmuth I**, **Nilsson KS**, **Tongiorgi P**, **Worsaae K**, **Todaro MA. 2012.** Patterns of diversity in soft-bodied meiofauna: dispersal ability and body size matter. *PLoS One* **7:** e33801.

Dayrat B. 2005. Towards integrative taxonomy. *Biological Journal of the Linnean Society* **85:** 407–415.

Diepenbroek M, **Glöckner F**, **Grobe P**, **Güntsch A**, **Huber R**, **König-Ries B**, **Kostadinov I**, **Nieschulze J**, **Seeger B**, **Tolksdorf R**, **Triebel D. 2014.** Towards an integrated biodiversity and ecological research data management and archiving platform: the German Federation for the Curation of Biological Data (GFBio). In: Plödereder E, Grunske L, Schneider E, Ull D, eds. *Informatik 2014 – Big Data Komplexität meistern. GI-Edition: Lecture Notes in Informatics (LNI) – Proceedings. GI edn. Vol. 232.* Bonn: Köllen Verlag, 1711–1724.

Edgar RC. 2004. MUSCLE: multiple sequence alignment with high accuracy and high throughput. *Nucleic Acids Research* **32:** 1792–1797.

Egger B, **Lapraz F**, **Tomiczek B**, **Müller S**, **Dessimoz C**, **Girstmair J**, **Skunca N**, **Rawlinson KA**, **Cameron CB**, **Beli E**, **Todaro MA**, **Gammoudi M**, **Noreña C**, **Telford MJ. 2015.** A transcriptomic-phylogenomic analysis of the evolutionary relationships of flatworms. *Current Biology* **25:** 1–7.

Felsenstein J. 1985. Confidence limits on phylogenies: an approach using the bootstrap. *Evolution* **39:** 783–791.

Folmer O, **Black M**, **Hoeh W**, **Lutz R**, **Vrijenhoek R. 1994.** DNA primers for amplification of mitochondrial cytochrome c oxidase subunit I from diverse metazoan invertebrates. *Molecular Marine Biology and Biotechnology* **3:** 294–299.

Garraffoni ARS, **Kieneke A**, **Kolicka M**, **Corgosinho PHC**, **Prado J**, **Nihei SS**, **Freitas AVL. 2019.** ICZN Declaration 45: a remedy for the nomenclatural and typification dilemma regarding soft-bodied meiofaunal organisms? *Marine Biodiversity* **49:** 2199–2207.

George KH. 2004. Description of two new species of *Bodinia*, a new genus incertae sedis in Argestidae Por, 1986 (Copepoda, Harpacticoida), with reflections on argestid colonization of the Great Meteor Seamount plateau. *Organisms, Diversity & Evolution* **4:** 241–264.

George KH. 2013. Faunistic research on metazoan meiofauna from seamounts – a review. *Meiofauna Marina* **20:** 1–32.

George KH, **Plum C. 2009.** Description of two new species of *Dorsiceratus* Drzycimski, 1967 (Copepoda: Harpacticoida: Ancorabolidae) from Sedlo and Seine Seamounts (northeastern Atlantic) and remarks on the phylogenetic status of the genus. *Zootaxa* **2096:** 257–286.

George KH, **Schminke HK. 2002.** Harpacticoida (Crustace, Copepoda) of the Great Meteor Seamount, with first conclusions as to the origin of the plateau fauna. *Marine Biology* **144:** 887–895.

George KH, **Arndt H**, **Wehrmann A**, **Baptista L**, **Berning B**, **Bruhn M**, **Carvalho F**, **Cordeiro R**, **Creemers M**, **Defise A**, **Domingues A**, **Hermanns K**, **Hohlfeld M**, **Iwan F**, **Janßen T**, **Jeskulke K**, **Kagerer M**, **Kaufmann M**, **Kieneke A**, **Loureiro C**, **Madeira P**, **Meyer C**, **Narciso ÁCM**, **Ostmann A**, **Pieper C**, **Pointner K**, **Raeke A**, **Silva T**, **Springer B**, **Wilsenack M. 2018.** Controls in benthic and pelagic BIODIversity of the Azores. *METEOR-Berichte Cruise No.* **M150:** 31–37.

Giere O. 2009. *Meiobenthology – the microscopic motile fauna of aquatic sediments.* Heidelberg: Springer.

Giribet G, **Sørensen MV**, **Funch P**, **Kristensen RM**, **Sterrer W. 2004.** Investigations into the phylogenetic position of Micrognathozoa using four molecular loci. *Cladistics* **20:** 1–13.

Guidi L, **Todaro MA**, **Ferraguti M**, **Balsamo M. 2014.** Reproductive system and spermatozoa ultrastructure support the phylogenetic proximity of *Megadasys* and *Crasiella* (Gastrotricha, Macrodasyida). *Contributions to Zoology* **83:** 119–131.

Hadziavdic K, **Lekang K**, **Lanzen A**, **Jonassen I**, **Thompson EM**, **Troedsson C. 2014.** Characterization of the 18S rRNA gene for designing universal eukaryote specific primers. *PLoS One* **9:** e87624.

Hamby RK, **Zimmer EA. 1988.** Ribosomal RNA sequences for inferring phylogeny within the grass family (Poaceae). *Plant Systematics and Evolution* **160:** 29–37.

Hebert PDN, **Ratnasingham S**, **De Waard JR. 2003.** Barcoding animal life: cytochrome c oxidase subunit I divergences among closely related species. *Proceedings of the Royal Society of London Series B* **270:** S96–S99.

Hillis DM, **Dixon MT. 1991.** Ribosomal DNA: molecular evolution and phylogenetic inference. *The Quarterly Review of Biology* **66:** 411–453.

Hummon WD. 2011. Marine Gastrotricha of the Near East: I. Fourteen new species of Macrodasyida and a redescription of *Dactylopodola agadasys* Hochberg, 2003. *ZooKeys* **94:** 1–59.

Hummon WD, Todaro MA. 2009. Italian marine Gastrotricha: VI. Seven new species of Macrodasyida. *Zootaxa* **2278:** 47–68.

Hummon WD, Todaro MA. 2010. Analytic taxonomy and notes on marine, brackish-water and estuarine Gastrotricha. *Zootaxa* **2392:** 1–32.

Hummon WD, Balsamo M, Todaro MA. 1992. Italian marine Gastrotricha: I. Six new and one redescribed species of Chaetonotida. *Bolletino di Zoologia* **59:** 499–516.

Hummon WD, Todaro MA, Tongiorgi P. 1993. Italian marine Gastrotricha: II. One new genus and ten new species of Macrodasyida. *Bollettino di Zoologia* **60:** 109–127.

Hummon WD, Todaro MA, Balsamo M, Tongiorgi P. 1996. Italian marine Gastrotricha: III. Four new pentancrous species of the genus *Tetranchyroderma* (Macrodasyida, Thaumastodermatidae). *Italian Journal of Zoology* **63:** 73–79.

Hummon WD, Todaro MA, Tongiorgi P, Balsamo M. 1998. Italian marine Gastrotricha: V. Four new and one redescribed species of Macrodasyida in the Dactylopodolidae and Thaumastodermatidae. *Italian Journal of Zoology* **65:** 109–119.

ICZN. 1999. *International code of zoological nomenclature, 4th edn.* London: International Trust for Zoological Nomenclature.

ICZN. 2017. Declaration 45 – addition of recommendations to article 73 and of the term 'specimen, preserved' to the Glossary. *Bulletin of Zoological Nomenclature* **73:** 96–97.

Kånneby T, Todaro MA, Jondelius U. 2012. A phylogenetic approach to species delimitation in freshwater Gastrotricha from Sweden. *Hydrobiologia* **683:** 185–202.

Kånneby T, Wicksten MK. 2014. First record of the enigmatic genus *Redudasys* Kisielewski, 1987 (Gastrotricha: Macrodasyida) from the Northern Hemisphere. *Zoosystema* **36:** 723–733.

Kieneke A. 2018. BIODIAZ – Die marine Geo- und Biodiversität der Azoren im Fokus. Forschung in der Mitte des Atlantiks. *GfBS Newsletter* **35:** 16–21.

Kieneke A, Nikoukar H. 2017. Integrative morphological and molecular investigation of *Turbanella hyalina* Schultze, 1853 (Gastrotricha: Macrodasyida), including a redescription of the species. *Zoologischer Anzeiger* **267:** 168–186.

Kieneke A, Schmidt-Rhaesa A. 2015. Gastrotricha. In: Schmidt-Rhaesa A, ed. *Handbook of zoology. Gastrotricha, Cycloneuralia and Gnathifera. Vol. 3: Gastrotricha and Gnathifera.* Berlin: De Gruyter, 1–134.

Kieneke A, Ahlrichs WH, Martínez Arbizu P. 2009. Morphology and function of reproductive organs in *Neodasys chaetonotoideus* (Gastrotricha: Neodasys) with a phylogenetic assessment of the reproductive system in Gastrotricha. *Zoologica Scripta* **38:** 289–311.

Kieneke A, Martínez Arbizu PM, Fontaneto D. 2012. Spatially structured populations with a low level of cryptic diversity in European marine Gastrotricha. *Molecular Ecology* **21:** 1239–1254.

Kieneke A, Bruhn M, George KH, Ostmann A, Wilsenack M. 2018. Meiofauna. In: George KH, ed. *METEOR-Berichte Cruise No. M150: controls in benthic and pelagic BIODIversity of the Azores.* Hamburg: Leitstelle Deutsche Forschungsschiffe, 31–37.

Kieneke A, Münter L, Riemann O. 2020. Gastrotricha. In: Schmidt-Rhaesa A, ed. *Guide to the identification of marine meiofauna.* Munich: Pfeil, 104–163.

Kisielewski J. 1990. Origin and phylogenetic significance of freshwater psammic Gastrotricha. *Stygologia* **5:** 87–92.

Koller S, George KH. 2011. Description of a new species of *Zosime* Boeck, 1872 (Copepoda: Harpacticoida: Zosimeidae) from the Great Meteor Seamount, representing one of the few eurybathic Harpacticoida among the distinct plateau and deepsea assemblages. *Meiofauna Marina* **19:** 109–126.

Kumar S, Stecher G, Li M, Knyaz C, Tamura K. 2018. MEGA X: molecular evolutionary genetics analysis across computing platforms. *Molecular Biology and Evolution* **35:** 1547–1549.

Lee JM. 2012. *Invertebrate fauna of Korea. Vol. 11, number 1, phylum Gastrotricha – marine gastrotrichs.* Incheon: National Institute of Biological Resources.

Lee JM, Chang CY. 2003. Two new marine gastrotrichs of the genus *Ptychostomella* (Macrodasyida, Thaumastodermatidae) from South Korea. *Zoological Science* **20:** 481–489.

MacArthur RH, Wilson EO. 1967. *The theory of island biogeography.* Princeton: Princeton University Press.

Martínez A, Di Domenico M, Leasi F, Curini-Galletti M, Todaro MA, Dal Zotto M, Gobert S, Artois T, Norenburg J, Jörger KM, Núñez J, Fontaneto D, Worsaae K. 2019. Patterns of diversity and endemism of soft-bodied meiofauna in an oceanic island, Lanzarote, Canary Islands. *Marine Biodiversity* **49:** 2033–2055.

Mioduchowska M, Czyż MJ, Goødyn B, Kur J, Sell J. 2018. Instances of erroneous DNA barcoding of metazoan invertebrates: are universal *cox1* gene primers too 'universal'? *PLoS One* **13:** e0199609.

Mueller RL. 2006. Evolutionary rates, divergence dates, and the performance of mitochondrial genes in bayesian phylogenetic analysis. *Systematic Biology* **55:** 289–300.

Nei M, Kumar S. 2000. *Molecular evolution and phylogenetics.* New York: Oxford University Press.

Nylander JAA. 2004. *MrModelTest 2.3. Program distributed by the author.* Uppsala: Uppsala University Evolutionary Biology Centre.

Page RDM. 1996. Tree View: an application to display phylogenetic trees on personal computers. *Bioinformatics* **12:** 357–358.

Petrov NB, Pegova AN, Manylov OG, Vladychenskaya NS, Mugue NS, Aleshin VV. 2007. Molecular phylogeny of Gastrotricha on the basis of a comparison of the 18S rRNA genes: rejection of the hypothesis of a relationship between Gastrotricha and Nematoda. *Molecular Biology* **41:** 445–452.

Pfannkuche O, Thiel H. 1988. Sample processing. In: Higgins RP, Thiel H, eds. *Introduction to the study of meiofauna.* Washington, DC: Smithsonian Institution Press, 134–145.

Plotnick RE, **Wagner PJ. 2006.** Round up the usual suspects: common genera in the fossil record and the nature of wastebasket taxa. *Palaeobiology* **32:** 126–146.

Ronquist F, **Huelsenbeck JP. 2003.** MrBayes 3: Bayesian phylogenetic inference under mixed models. *Bioinformatics* **19:** 1572–1574.

Rueden CT, **Schindelin J**, **Hiner MC**, **DeZonia BE**, **Walter AE**, **Arena ET**, **Eliceiri KW. 2017.** ImageJ2: ImageJ for the next generation of scientific image data. *BMC Bioinformatics* **18:** 529.

Ruppert EE. 1978. The reproductive system of gastrotrichs. III. Genital organs of Thaumastodermatinae subfam. n. and Diplodasyinae subfam. n. with discussion of reproduction in Macrodasyida. *Zoologica Scripta* **7:** 93–114.

Ruppert EE, **Shaw K. 1977.** The reproductive system of gastrotrichs. I. Introduction with morphological data for two new *Dolichodasys* species. *Zoologica Scripta* **6:** 185–195.

Saitou N, **Nei M. 1987.** The neighbor-joining method: a new method for reconstructing phylogenetic trees. *Molecular Biology and Evolution* **4:** 406–425.

Schindelin J, **Arganda-Carreras I**, **Frise E**, **Kaynig V**, **Longair M**, **Pietzsch T**, **Preibisch S**, **Rueden C**, **Saalfeld S**, **Schmid B**, **Tinevez J-Y**, **White DJ**, **Hartenstein V**, **Eliceiri K**, **Tomancak P**, **Cardona A. 2012.** Fiji: an open-source platform for biological-image analysis. *Nature Methods* **9:** 676–682.

Schmidt P. 1974. Interstitielle fauna von Galapagos IV. Gastrotricha, *Mikrofauna des Meeresbodens* **26:** 1–76.

Schmidt-Rhaesa A. 2013. Gastrotricha, Cycloneuralia and Gnathifera: general history and phylogeny. In: Schmidt-Rhaesa A, ed. *Handbook of zoology. Gastrotricha, Cycloneuralia and Gnathifera. Vol. 1: Nematomorpha, Priapulida, Kinorhyncha and Loricifera.* Berlin: De Gruyter, 1–10.

Schoepfer-Sterrer C. 1974. Five new species of *Urodasys* and remarks on the terminology of the genital organs in Macrodasyidae (Gastrotricha). *Cahiers de Biologie Marine* **15:** 229–254.

Sørensen MV, **Sterrer W**, **Giribet G. 2006.** Gnathostomulid phylogeny inferred from a combined approach of four molecular loci and morphology. *Cladistics* **22:** 32–58.

Struck TH, **Wey-Fabrizius AR**, **Golombek A**, **Lars Hering L**, **Weigert A**, **Bleidorn C**, **Klebow S**, **Iakovenko N**, **Hausdorf B**, **Petersen M**, **Kück P**, **Herlyn H**, **Hankeln T. 2014.** Platyzoan paraphyly based on phylogenomic data supports a noncoelomate ancestry of Spiralia. *Molecular Biology and Evolution* **31:** 1833–1849.

Thompson JD, **Higgin DG**, **Gibson TJ. 1994.** CLUSTAL W: improving the sensitivity of progressive multiple sequence alignment through sequence weighting, position-specific gap penalties and weight matrix choice. *Nucleic Acids Research* **22:** 4673–4680.

Todaro MA. 2002. An interesting new gastrotrich from littoral meiobenthos (Long Beach Island, USA), with a key to species of *Tetranchyroderma* (Gastrotricha: Macrodasyida). *Journal of the Marine Biological Association of the UK* **82:** 555–563.

Todaro MA. 2013. A new non-naked species of *Ptychostomella* (Gastrotricha) from Brazil. *ZooKeys* **289:** 13–24.

Todaro MA, **Hummon WD. 2008.** An overview and a dichotomous key to genera of the phylum Gastrotricha. *Meiofauna Marina* **16:** 3–20.

Todaro MA, **Balsamo M**, **Tongiorgi P. 2002.** Marine gastrotrich fauna in Corsica (France), with a description of a new species of the genus *Tetranchyroderma* (Macrodasyida, Thaumastodermatidae). *Sarsia* **87:** 248–257.

Todaro MA, **Telford MJ**, **Lockyer AE**, **Littlewood DTJ. 2006.** Interrelationships of Gastrotricha and their place among the Metazoa inferred from 18S rRNA genes. *Zoologica Scripta* **35:** 251–259.

Todaro MA, **Kånneby T**, **Dal Zotto M**, **Jondelius U. 2011.** Phylogeny of Thaumastodermatidae (Gastrotricha: Macrodasyida) inferred from nuclear and mitochondrial sequence data. *PLoS One* **6:** e17892.

Todaro MA, **Dal Zotto M**, **Jondelius U**, **Hochberg R**, **Hummon WD**, **Kånneby T**, **Rocha CEF. 2012.** Gastrotricha: a marine sister for a freshwater puzzle. *PLoS One* **7:** e31740.

Todaro MA, **Leasi F**, **Hochberg R. 2014.** A new species, genus and family of marine Gastrotricha from Jamaica, with a phylogenetic analysis of macrodasyida based on molecular data. *Systematics and Biodiversity* **12:** 473–488.

Todaro MA, **Dal Zotto M**, **Leasi F. 2015.** An integrated morphological and molecular approach to the description and systematisation of a novel genus and species of Macrodasyida (Gastrotricha). *PLoS One* **10:** e0130278.

Todaro MA, **Sibaja-Cordero JA**, **Segura-Bermúdez OA**, **Coto-Delgado G**, **Goebel-Otárola N**, **Barquero JD**, **Cullell-Delgado M**, **Dal Zotto M. 2019a.** An introduction to the study of Gastrotricha, with a taxonomic key to families and genera of the group. *Diversity* **11:** 117.

Todaro MA, **Dal Zotto M**, **Kånneby T**, **Hochberg R. 2019b.** Integrated data analysis allows the establishment of a new, cosmopolitan genus of marine Macrodasyida (Gastrotricha). *Scientific Reports* **9:** 7989.

Todaro MA, **Cesaretti A**, **Dal Zotto M. 2019c.** Marine gastrotrichs from Lanzarote, with a description of a phylogenetically relevant species of *Urodasys* (Gastrotricha, Macrodasyida). *Marine Biodiversity* **49:** 2109–2123.

Valbonesi A, **Luporini P. 1984.** Researches on the coast of Somalia. Gastrotricha Macrodasyoidea. *Italian Journal of Zoology* **19:** 1–34.

Wilke U. 1954. Mediterrane Gastrotrichen. Zoologische Jahrbücher. *Abteilung für Systematik, Ökologie und Geographie der Tiere* **82:** 497–550.

WoRMS Editorial Board. **2020.** *World register of marine species.* Available at: http://www.marinespecies.org at VLIZ (accessed 18 March 2020), doi: 10.14284/170.

Yamauchi S, **Kajihara H. 2018.** Marine Macrodasyida (Gastrotricha) from Hokkaido, northern Japan. *Species Diversity* **23:** 183–192.

SUPPORTING INFORMATION

Additional Supporting Information may be found in the online version of this article at the publisher's web-site.

Figure S1. Tree with the highest log-likelihood (−11 934.06) from the maximum likelihood (ML) search based on the *COI* gene alignment of 72 gastrotrich sequences of 39 species using the GTR+I+G model for nucleotide substitution. Averaged branch lengths are proportional to substitutions per site under the used model. Support values form the bootstrap test (1000 replications) are provided next to branches or corresponding nodes, respectively. Highlighted bootstrap values (black squares) indicate the good support of most species represented by more than a single sequence and many genera represented by more than a single species. Evolutionary analyses were conducted in MEGA X (Kumar *et al.*, 2018). Grey boxes indicate sequences of Thaumastodermatidae.

Table S1. Gastrotrich *COI* mtDNA sequences used in the phylogenetic analyses. Species, accession numbers, geographic origin and reference. Accession numbers marked with an asterisk (*) are tagged as 'COI-like' and are possibly mitochondrially derived nuclear genes.